UNIVERSIDADE DE LISBOA
FACULDADE DE CIÊNCIAS
DEPARTAMENTO DE FÍSICA

Continuous Monitoring of Vital Parameters for Clinically Valid Assessment of Human Health Status

Neusa Rebeca Adão Martins

Mestrado Integrado em Engenharia Biomédica e Biofísica
Perfil Sinais e Imagens Médicas

Dissertação orientada por:
Dr. Alexandre Andrade
Dr. Simon Annaheim

2019

Acknowledgments

First, I would like to express my deepest gratitude to God, for all He is and has done for me.

Many thanks to my family. Words cannot describe my thankfulness for your support, care and love throughout my academic journey.

A special thanks to my supervisors, Alexandre Andrade and Simon Annaheim. Thank you very much for your support, guidance and constructive criticism during the entire process of producing this dissertation.

I would also like to acknowledge the valuable contribution of Isabelle Gentgen, Claire Guignier, Dario, Martin Camenzind, Michel Schmid, Piero Fontana and Patrick Eggenberger, to this work.

Abstract

The lack of devices suitable for acquiring accurate and reliable measures of patients' physiological signals in a remote and continuous manner together with the advances in data acquisition technologies during the last decades, have led to the emergence of wearable devices for healthcare. Wearable devices enable remote, continuous and long-term health monitoring in unattended setting. In this context, the Swiss Federal Laboratories for Material Science and Technology (Empa) developed a wearable system for long-term electrocardiogram measurements, referred to as textile belt. It consists of a chest strap with two embroidered textile electrodes. The validity of Empa's system for electrocardiogram monitoring has been proven in a clinical setting. This work aimed to assess the validity of the textile belt for electrocardiogram monitoring in a home setting and to supplement the existing system with sensors for respiratory monitoring. Another objective was to evaluate the suitability of the same wearable, as a multi-sensor system, for activity monitoring.

A study involving 12 patients (10 males and 2 females, interquartile range for age of 48–59 years and for body mass indexes of 28.0–35.5 $kg.m^{-2}$) with suspected sleep apnoea was carried out. Overnight electrocardiogram was measured in a total of 28 nights. The quality of recorded signals was assessed using signal-to-noise ratio, artefacts detection and Poincaré plots. Study data were compared to data from the same subjects, acquired in the clinical setting. For respiratory monitoring, optical fibre-based sensors of different geometries were integrated into the textile belt. Signal processing algorithms for breathing rate and tidal volume estimation based on respiratory signals acquired by the sensors were developed. Pilot studies were conducted to compare the different approaches for respiratory monitoring. The quality of respiratory signals was determined based on signal segments "sinusoidality", evaluated through the calculation of the cross-correlation between signal segments and segment-specific reference waves. A method for accelerometry-based lying position recognition was proposed, and the proof of concept of activity intensity classification through the combination of subjects' inertial acceleration, heart rate and breathing rate data, was presented. Finally, a study with three participants (1 male and 2 females, aged 21 ± 2 years, body mass index of 20.3 ± 1.5 $kg.m^{-2}$) was conducted to assess the validity of the textile belt for respiratory and activity monitoring.

Electrocardiogram signals acquired by the textile belt in the home setting were found to have better quality than the data acquired by the same device in the clinical setting. Although a higher artefact percentage was found for the textile belt, signal-to-noise ratio of electrocardiogram signals recorded by the textile belt in the home setting was similar to that of signals acquired by the gel electrodes in the clinical setting. A good agreement was found between the RR-intervals derived from signals recorded in home and clinical settings. Besides, for artefact percentages greater than 3%, visual assessment of Poincaré plots proved to be effective for the determination of the primary source of artefacts (noise or ectopic beats).

Acceleration data allowed posture recognition (i.e. lying or standing/sitting, lying position) with an accuracy of 91% and positive predictive value of 80%. Lastly, preliminary results of physical activity intensity classification yielded high accuracy, showing the potential of the proposed method.

The textile belt proved to be appropriate for long-term, remote and continuous monitoring of subjects' physical and physiological parameters. It can monitor not only electrocardiogram, but also breathing rate, body posture and physical activity intensity, having the potential to be used as tool for disease prediction and diagnose support.

Keywords: long-term electrocardiogram; respiratory monitoring; fibre optic sensing; activity monitoring; home monitoring.

Resumo

Contexto: A falta de dispositivos adequados para a monitorização de sinais fisiológicos de um modo remoto e contínuo, juntamente com avanços tecnológicos na área de aquisição de dados nas últimas décadas, levaram ao surgimento de *wearable devices*, i.e. dispositivos vestíveis, no sector da saúde. *Wearable devices* possibilitam a monitorização do estado de saúde, de uma forma remota, contínua e de longa duração. Quando feito em ambiente domiciliar, este tipo de monitorização (i.e. contínua, remota e de longa duração) tem várias vantagens: diminui a pressão posta sobre o sistema de saúde, reduz despesas associadas ao internamento e acelera a resposta a emergências, permitindo deteção precoce e prevenção de condições crónicas. Neste contexto, a Empa, Laboratórios Federais Suíços de Ciência e Tecnologia de Materiais, desenvolveu um sistema vestível para a monitorização de eletrocardiograma de longa duração. Este sistema consiste num cinto peitoral com dois elétrodos têxteis integrados. Os elétrodos têxteis são feitos de fio de polietileno tereftalato revestido com prata e uma ultrafina camada de titânio no topo. De modo a garantir a aquisição de sinais de alta qualidade, o cinto tem nele integrado um reservatório de água que liberta vapor de água para humidificar os elétrodos. Este reservatório permite a monitorização contínua de eletrocardiograma por 5 a 10 dias, sem necessitar de recarga. A validade do cinto para a monitorização de eletrocardiograma em ambiente clínico já foi provada.

Objetivo: Este trabalho teve por objetivo avaliar a validade do cinto para a monitorização de eletrocardiograma em ambiente domiciliar e complementar o sistema existente com sensores para monitorização respiratória. Um outro objetivo foi analisar a adequação do cinto, como um sistema multisensor, para monitorização da atividade física.

Métodos: Um estudo com 12 pacientes com suspeita de apneia do sono (10 homens e 2 mulheres, amplitude interquartil de 48–59 anos para a idade e de 28.0–35.5 $kg.m^{-2}$ para o índice de massa corporal) foi conduzido para avaliar a qualidade do sinal de eletrocardiograma medido em ambiente domiciliar. O sinal de eletrocardiograma dos pacientes foi monitorizado continuamente, num total de 28 noites. A qualidade dos sinais adquiridos foi analisada através do cálculo da razão sinal-ruído; da deteção de artefactos, i.e., intervalos RR com um valor inviável de um ponto de vista fisiológico; e de gráficos de Poincaré, um método de análise não linear da distribuição dos intervalos RR registados. Os dados adquiridos neste estudo foram comparados com dados dos mesmos pacientes, adquiridos em ambiente hospitalar.

Para a monitorização respiratória, sensores feitos de fibra óptica foram integrados no cinto. Algorítmicos para a estimar a frequência respiratória e o volume corrente dos sujeitos tendo por base o sinal medido pelas fibras ópticas foram desenvolvidos neste trabalho. As diferentes abordagens foram comparadas através de estudos piloto. Diferentes métodos para avaliação da qualidade do sinal adquirido foram sugeridos.

Um método de reconhecimento da postura corporal através do cálculo de ângulos de orientação com base na aceleração medida foi proposto. A prova de conceito da determinação da intensidade da atividade física pela combinação de informações relativas á aceleração inercial e frequências cardíaca e respiratória dos sujeitos, é também apresentada neste trabalho. Um estudo foi conduzido para avaliar a validade do cinto para monitorização da respiração e da atividade física. O estudo contou com 10 participantes, dos quais 3 vestiram o cinto para monitorização da respiração (1 homem e 2 mulheres, idade 21 ± 2 anos, índice de massa corporal 20.3 ± 1.5 $kg.m^{-2}$).

Resultados: O estudo feito com pacientes com suspeita de apneia do sono revelou que os sinais eletrocardiográficos adquiridos pelo cinto em ambiente domiciliar foram de melhor qualidade que os sinais adquiridos pelo mesmo dispositivo em ambiente hospitalar. Uma percentagem de artefacto de 2.87% ±

4.14% foi observada para os dados adquiridos pelos elétrodos comummente usados em ambiente hospitalar, 7.49% ± 10.76% para os dados adquiridos pelo cinto em ambiente domiciliar e 9.66% ± 14.65% para os dados adquiridos pelo cinto em ambiente hospitalar. Embora tenham tido uma maior percentagem de artefacto, a razão sinal-ruído dos sinais eletrocardiográficos adquiridos pelo cinto em ambiente domiciliar foi semelhante á dos sinais adquiridos pelos elétrodos de gel em ambiente hospitalar. Resultados sugerem uma boa concordância entre os intervalos RR calculados com base nos eletrocardiogramas registados em ambientes hospitalar e domiciliar. Além disso, para sinais com percentagem de artefacto superior a 3%, a avaliação visual dos gráficos de Poincaré provou ser um bom método para a determinação da fonte primária de artefactos (batimentos irregulares ou ruído).

A monitorização da aceleração dos sujeitos permitiu o reconhecimento da postura corporal (isto é, deitado ou sentado/em pé) com uma exatidão de 91% e valor preditivo positivo de 80%. Por fim, a classificação da intensidade da atividade física baseado na aceleração inercial e frequências cardíaca e respiratória revelou elevada exatidão, mostrando o potencial desta técnica.

Conclusão: O cinto desenvolvido pela Empa provou ser apropriado para monitorização de longa-duração de variáveis físicas e fisiológicos, de uma forma remota e contínua. O cinto permite não só monitorizar eletrocardiograma, mas também frequência respiratória, postura corporal e intensidade da atividade física. Outros estudos devem ser conduzidos para corroborar os resultados e conclusões deste trabalho. Outros sensores poderão ser integrados no cinto de modo a possibilitar a monitorização de outras variáveis fisiológicas de relevância clínica. Este sistema tem o potencial de ser usado como uma ferramenta para predição de doenças e apoio ao diagnóstico.

Palavras-chave: eletrocardiograma de longa duração; monitorização da respiração; sensorização por fibra óptica; monitorização da atividade física; monitorização em casa.

Contents

List of Figures

List of Tables

List of Abbreviations and Acronyms

ACSM	American College of Sports Medicine
AHI	Apnea-hypopnea index
AUC	Area under the curve
BLW	Baseline wander
BMI	Body mass index
bpm	Beats per minute
BR	Breathing rate
CE	Conformité Européenne
dBc	Decibels relative to the carrier
DLW	Doubly labeled water
ECG	Electrocardiogram
EE	Energy expenditure
Empa	Swiss Federal Laboratories for Material Science and Technology
FBG	Fiber Bragg grating
FDA	Food and Drug Administration
FFT	Fast Fourier transform
FOS	Fiber optic sensor
HR	Heart rate
HRV	Heart rate variability
ICU	Intensive care unit
LED	Light-emitting diode
LoA	Limits of agreement
LPG	Long period granting
MAE	Mean absolute error
MAPE	Mean absolute percentage error
MET	Metabolic equivalent of the task
mg	Milligravity
MRI	Magnetic resonance imaging
PPG	Photoplethysmography
PPV	Positive predictive value
PSG	Polysomnography
RIP	Respiratory inductive plethysmography
ROC	Receiver-operating characteristic
RPE	Rating of perceived exertion
SD	Standard deviation
SEE	Standard error of estimates
SNR	Signal-to-noise ratio
SQA	Signal quality assessment
TEE	Total energy expenditure
TV	Tidal volume
USB	Universal serial bus
WHO	World Health Organization

1. INTRODUCTION

1.1. Project scope and research plan

The lack of devices suitable for acquiring accurate and reliable measures of patients' physiological signals in a remote and continuous manner together with the advances in data acquisition technologies during the last decades, has led to the emergence of wearable devices for healthcare. Within this field, the use of textile-based sensors is valuable as it enables unobtrusive and comfortable means of measurement, while allowing long-term monitoring.

Remote, continuous health monitoring in unattended setting has many advantages: decreases pressure on health systems, reduces expenses associated with inpatient care and accelerates the response to emergencies while enabling early detection and prevention of chronic conditions. However, the lack of confidence in the quality of the signal acquired and its clinical relevance, the need to acquire and process large amount of data as well as the need to combine simplicity of use and robustness against artifacts while ensuring acceptable integration in user's daily life, data security and data privacy, are some of the main challenges within this field.

Long-term health monitoring also requires systems with low power consumption and high energy efficiency and, when done by means of wearable sensors, the durability and signal integrity of the sensors with time and cleaning process must be ensured. Most of the proposed systems consider only a specific physiological signal or parameter. However, the use of several wearable devices to monitor different physiological parameters is neither practical nor ergonomically sound; therefore, developing multi-sensor monitoring systems is desirable.

With that knowledge in mind, the Swiss Federal Laboratories for Material Science and Technology (Empa) aim to develop a wearable monitoring system that enables continuous and non-invasive monitoring of multiple vital parameters, fulfilling accuracy requirements to be used in clinical settings. At this point, the system consists of a textile belt with integrated sensors combining own technologies, such as embroidered electrodes with Silver/Titanium coating for ECG monitoring [1] and optical fibre-based sensor for respiratory monitoring [2], with commercially available sensors, giving rise to the concept of "lab on the belt".

The parameters of interest are respiratory rate; electrocardiogram (ECG) and RR-intervals based on the former; body posture, physical activity, movement patterns and energy expenditure; and, lastly, blood oxygen saturation (SpO_2), since all these parameters can be measured from the skin surface.

Respiratory rate, also called breathing rate, is one of the four classic vital signs, crucial to determine subjects' health status. It is used in the diagnosis of sepsis/ septic shock, sleep related breathing disorders, such as sleep apnea, and many other conditions. Likewise, ECG is essential in the diagnosis of cardiovascular diseases, the main cause of death globally according to the World Health Organization (WHO). Additionally, continuous ECG monitoring is used in intensive care unit (ICU) to monitor critically ill patients. Thus, due to their clinical relevance, these two parameters will be our focus of research.

Furthermore, body posture and physical activity is taken into account, since it has been shown its suitability not only for fall detection in elderly care, but also for assistance of patients suffering from neurodegenerative disorders, motor diseases and cancer.

Within this framework, this master thesis project intended to answer the following questions:

1) How accurate is the ECG data recorded without supervision in home setting?
2) Is it possible to accurately and continuously monitor breathing through the integration of optical fibre into the belt?
    a. If yes, is it possible to measure respiratory rate?
    b. And tidal volume?

3) Is it possible to accurately recognize lying positions/ body postures/ activities/ activity patterns from accelerometry data?

1.2. State of the art

Devices currently used in clinical practice for the assessment of patients' health status enable accurate measurement of physiological parameters, yet they are not suitable for continuous ambulatory monitoring. Even though continuous monitoring of vital signs, such as ECG and breathing rate, is applied to patients in ICUs, the vital signs of patients that are not in a critical condition are measured intermittently. However, patients' health status may degrade in the time between measurements. Standard medical devices used for diagnosis provide a "snapshot in time"[3] of patients' health status. Nevertheless, relevant events may not occur during the examination, as might be the case in patients suffering from rare occurring arrhythmias [4]; and the presence of a healthcare professional may induce changes in patients vital signs, as happens in white coat effect (i.e. increase in blood pressure associated with clinical visit [5]). Therefore, there is a need for medical devices enabling long-term, remote and continuous monitoring.

The suitability of wearable devices for remote, continuous and long-term monitoring of physiological parameters makes of such a technology the focus of study of many researchers, especially nowadays. Over the past decades, it has been observed a gradual increase in life expectancy worldwide simultaneously with declining birth rates. This phenomenon results in population aging, which requires a considerable economic investment in order to provide the assistance needed to elderly, especially concerning healthcare [6].

Wearable devices are any device a subject can "wear without encumbering daily activities or restricting mobility" [3]. Sensors have been integrated in clothes (T-shirts, bras, socks, pants), watches, chest straps, elastic bands, patches, tags, glasses etc., ensuring continuous monitoring with the maximum wear comfort and minimum interference in subjects' daily activities [3]. There is a wide range of application fields of wearable devices [3], [6]–[9]:

- Healthcare: monitoring for disease prediction, anomaly detection, recovery, rehabilitation, diagnosis support;
- Assistive living;
- Surveillance and security: monitoring of subjects in risky situations (e.g. solders, firefighters or astronauts);
- Fitness/Sport: monitoring of physical and physiological parameters to improve performance or increase wellness;
- Human computer interaction and robotics.

To be used in healthcare, wearable devices must satisfy various medical and ergonomic requirements. They must be of small dimension, comfortable, its components should be flexible, chemically inert, nontoxic, and hypoallergenic to the human body. For the successful commercialization, it should also be low-cost, lightweight, user-friendly, unobtrusive (should not require the user to wear many sensors), non-invasive and, additionally, the whole system should not require user interaction too often [6], [8], [9].

Depending on their application, wearable devices can be used to monitor healthy subjects and patients, in home or clinical environment. Data can be stored locally on the wearable device (in the data-logger unit) or be transmitted, via Bluetooth, Wi-Fi, ZigBee or long range radio, to receiving devices where it is displayed in real-time, or even to a remote monitoring center. While offline monitoring is adequate for disease prediction and diagnose support, it is not appropriate for activity monitoring or

anomaly detection (e.g. fall, seizure, or cardiac arrest detection), as both require real-time feedback (e.g. alarms) to medical staff and wearer [3], [10].

The monitored bio signals and physiological parameters include ECG, heart rate (HR), electroencephalogram, electromyogram, gait patterns, minute ventilation, breathing rate, breathing pattern, air quality, physical activity, arterial oxygen saturation, blood pressure, blood glucose, skin perspiration, galvanic skin response, capnography and body temperature [3], [6], [10], [11]. The sensor most widely used in wearable devices is the accelerometer [11].

A huge number of wearable devices are available on the market; however, the reliability, accuracy, safety and efficacy of the vast majority has not been proved. In fact, only an extremely reduced fraction of existing wearable devices are CE (Conformité Européenne) or FDA (Food and Drug Administration) approved [3]. CE [12] and FDA [13] definitions of medical devices clearly include wearable devices for healthcare applications. Thus, most commercially available wearable devices cannot be commercialized as medical devices, as they do not have a mark of conformity.

Wearable devices market has been constantly growing, being estimated that its total worth is over $50 billion this year [14]. Wearables for lifestyle, fitness and sport applications are predominant in this market. The market of wearable devices for healthcare applications is also growing, however, the lack of confidence in the quality of the acquired signal on the part of clinicians as well as the requirements in terms of device certification have been hindering its growth [10], [11].

A summary on the standard devices as well wearable devices used for ECG, breathing and physical activity monitoring is presented in the following sections.

1.2.1.ECG monitoring

The surface ECG is a continuous record of voltage changes, generated as a response of cardiac muscles to electrical impulses generated by pacemaker cells [15]. In this way, the ECG reflects the cyclic electro-physiologic events in the myocardium, revealing the condition of heart's electrical function [16]. It has a preponderant role in detection of heart defects and cardiac diseases such as auricular or ventricular hypertrophy, myocardial infarction (heart attack), arrhythmias and pericarditis. It also allows the analysis of heart rate variability (HRV), a straightforward way to study the autonomic nervous system activity. ECG signals are acquired by means of electrodes.

Today's gold standard for ECG recording are the gel electrodes. However, these electrodes have a limited application period, i.e. one or maximum two days, since they tend to run dry as the moisture content evaporates, and cause skin irritations on long-term use, apart from being uncomfortable for users [1], [17].

Generally, biopotential electrodes can be categorized in three groups: wet, dry and non-contact electrodes. Wet electrodes are the most common type, being the gold standard for clinical applications. Gel electrodes belong to this class. They consist of a metal (e.g. silver or gold) surrounded by a wet or solid hydrogel that is coupled to the skin (galvanic coupling). Dry electrodes operate without the use of an explicit moisturizing substance. Instead, the metal in the electrode directly contacts the skin using only some degree of moisture coming from the environment or emitted from the body (e.g. sweat). Their performance usually increases over time with increasing moisture between the electrode and the skin, as it reduces the electrode-skin impedance. There are also dry contact electrodes with capacitive coupling, in which a thin dielectric layer is used to form an insulated contact with the body. Such electrodes measure electric surface potentials on the skin by the principle of electrostatic induction. The non-contact electrodes are a particular case of dry electrodes. They function without being in direct contact with skin. Non-contact electrodes enable data acquisition through an insulation layer such as clothing [17]. Although dry electrodes enable long-term ECG monitoring, to be used for clinical purposes their performance must match that of gel electrodes.

Textile electrodes, made from textile fibers with conductive properties, have also been used as an alternative to gel electrodes. They are flexible, adjusting easily to body topography, and can be unobtrusively integrated into a garment. Additionally, air and moisture can pass through the porous textile electrodes, decreasing the risk for skin inflammation and increasing users' comfort. However, data acquired by textile electrodes is more susceptible to motion artefacts as electrodes can easily move relative to the skin. Ensuring electrodes integrity and durability as well as cope with the electric performance variation of such electrodes are among the greatest challenges in the field of textile electrodes for ECG monitoring [18].

The most popular device for long-term, ambulatory monitoring of ECG is the Holter™ ECG Recorder. It is a 12-lead wearable device that allows remote and continuous ECG monitoring up to 3 days [11], [19]. However, Holter monitors use conventional gel electrodes. Efforts have been made to develop wearable systems using different types of electrodes and with fewer leads, thus increasing comfort and unobtrusiveness, while increasing the monitoring time. Several wearable systems for long-term ECG monitoring, mainly chest straps, t-shirts and adhesive patches [10], have been proposed.

Table 1.1 presents some of the existing wearable devices for ECG monitoring. From the systems presented, the first four are commercially available, while the other four were proposed in literature. Zio, developed by iRhythm, is a patch able to monitor ECG for up to two weeks. Nuubo is a chest strap with integrated textile electrodes for long-term ECG-monitoring. Both are currently in use for clinical applications. Zoll LifeVest is a wearable cardioverter defibrillator that monitors ECG. It has been used to monitor patients at risk of sudden cardiac death.

Table 1.1. Wearable devices for remote, continuous and long-term ECG monitoring. CF: compact flash; LE: low energy; GMS: Global System for Mobile communications; ANT: Adaptive Network Topology.

System/ Proposition	Number of electrodes	Electrode type	Sensors Placement	Battery Life	Connectivity	Market Clearance
Holter Recorder [19]	12	Wet electrodes	Ventral Trunk	3 days	CF card	FDA and CE
Zio Patch [20]	2	Hydrogel electrodes	Chest	14 days	Wireless	FDA
Zoll LifeVest [21]	2	Dry electrodes	Chest	1 day	Wireless	FDA
Nuubo [22]	2	Textile electrodes	Chest	5 days	Wireless (Bluetooth LE)	FDA and CE
Sensorized T-shirt and textile belt [23]	3	Dry textile electrodes	Chest	-	Wireless (Bluetooth LE)	-
Wearable mobile electrocardiogram monitoring system [24]	3	Dry foam electrodes	Chest	-	Wireless (Bluetooth and GSM)	-
Wireless, portable capacitive ECG sensor [25]	3	Capacitive electrodes with cotton insulator	Ventral Trunk	-	Wireless (ANT protocol)	-
Flexible capacitive electrodes for reducing motion artifacts [26]	2	Flexible capacitive electrodes	Chest	-	Wireless (Bluetooth)	-

1.2.1.1. Textile Belt for Long-Term ECG monitoring

Empa developed a system for long-term ECG measurements. It consists of a textile belt (Unico Swiss Tex GmbH, Alpnachstad, Switzerland) with two embroidered textile electrodes from polyethylene terephthalate yarn, which are plasma coated with silver and with an ultra-thin titanium layer on top. The belt has stretchable parts and trims to ensure good electrode-skin contact for different body sizes, as shown in Figure 1.1.

Since it was proved that humidification improves the signal quality in motion, electrodes are moisturized with a very low amount of water vapor from an integrated reservoir [1]. The integrated reservoir is composed of a wetting pad made from polyester that is impermeable to liquid water but allows the passage of water vapor. The wetting pad is connected to a flexible water tank and releases a small amount of water that evaporates mainly due to body heat of the wearer. The water vapor permeates the membranes of the wetting pad thus creating a favorable silver-titanium-water electrode chemistry due to a high relative humidity atmosphere. This atmosphere prevents artifacts that results from the friction between electrode and skin, allowing the acquisition of good quality signal with baseline stability even when there are large body motions during the measurement. The water reservoir allows continuous ECG recording over 5-10 days without a refill.

Figure 1.1. Textile belt connected to data logger (red device). Front (top) and back (bottom) view.

Electrodes measures are stored in a data logger. The validity, reliability and clinical relevance of this system are being tested by means of experiments with volunteers and clinical trials [27], [28].

1.2.2. Respiratory Monitoring

At present, respiratory rate monitoring is done in a continuous manner only in ICUs. On general hospital wards, nurses measure it intermittently only. They do it manually, counting the number of breaths, based on patient's chest movement, during a minute. Apart of being a time-consuming task, it is hard to apply this methodology to non-cooperative patients. Consequently, breathing rate is the most neglected vital sign and its value is sometimes simply estimated or even guessed [29], [30].

Respiratory rate is an early indicator of patient's health status deterioration since the compensatory mechanisms normally first increase heart and respiratory rates. It is valuable to recognize acute changes in patients' condition, especially when measured in a continuous manner, as patient's health status can drastically change in the gaps between measurements when an intermittent methodology is followed. Respiratory rate increases in hypovolemia and increased respiratory rate can be an early marker of acidosis. Additionally, abnormal respiratory rate is common prior to cardiac arrest [29]. Measuring tidal volume is also important when it comes to respiratory monitoring. Tidal volume is the volume of air that is inhaled and exhaled with each breath. Abnormalities in its value are related with asthma, pneumonia and chronic obstructive pulmonary disease.

Respiratory rate and tidal volume are calculated from the respiratory signal acquired through different techniques. The clinical standard techniques for respiratory monitoring include capnography, spirometry, impedance pneumography, and respiratory inductive plethysmography (RIP). Capnography, also called end-tidal CO_2 monitoring, is the standard for respiratory monitoring in ICUs and in the operating room. It is the measurement of CO_2 concentration in exhaled air over time [31]. Spirometry is the gold standard for tidal volume measurement [32]. Even though it is an accurate method, it is also invasive. During spirometry, the patient must breathe through a tube while wearing a nose clip or a face mask. Thus, such device is not suitable for continuous monitoring. It is uncomfortable and alters patient’s natural breathing behaviors.

Impedance pneumography consists in measuring changes in transthoracic impedance as a function of respired volume using superficial thoracic electrodes [33], [34]. Pairs of electrodes (usually one or two [35]), one injecting current and other measuring voltage changes, are placed on the subject’s thorax to measure its impedance. Research has been conducted to find the optimal electrodes configuration, increasing accuracy and reducing obtrusiveness [36]. It is the clinical standard for electronic breathing

rate measurement [37]. It has been used during overnight polysomnography (PSG), the gold standard for the diagnosis of sleep related disorders [38], to monitor respiratory effort.

RIP enables non-invasive respiratory monitoring by measuring the movement of the chest and abdominal wall. Two inductance sensors (coils) integrated into elastic bands, one placed at the level of nipples and other at the level of umbilicus, are deployed to monitor respiratory movements. Respiratory movements cause changes on the surface encircled by the sensors, altering the current induced by magnetic field in the coils [39], [40]. Output signal must be calibrated to measure volume. RIP devices are standard in clinical environment. Due to their portability, ambulatory RIP has been proposed [39][41], however body posture changes invalidate calibration. Thus, for volume measurement, recalibration is required each time subjects' body position changes. Brüllmann et al.[40] proposed an accelerometry-based approach to solve the recalibration problem. Another study suggest that ambulatory RIP is a reliable method for respiratory monitoring [42].

A review on the existing contact methods for measuring respiratory rate is presented in by Massaroni et al. [35]. They categorized the sensing principles for respiratory monitoring in seven groups:

1) Respiratory airflow: measurement of the volume or velocity of inhaled and exhaled air using flowmeters. This method enables accurate breathing rate estimation but is intrusive, as usually implies use of face mask.
2) Respiratory sounds: recording of respiratory sounds using microphones. This approach enables monitoring with reduced encumbrance, being suitable to be applied in wearable devices. However, its use is not recommended as microphones can easily record sounds that are not related to breathing.
3) Air temperature: measurement of the difference between the temperature of inhaled and exhaled air, as inhaled air is at ambient temperature, while exhaled air is warmer. Thermistors, thermocouples, pyroelectric sensors and optical fibres have been used for this purpose. This approach is sensitive to environmental factors, intrusive and not suitable for ambulatory monitoring.
4) Air humidity: measurements of the water vapor content of inhaled and exhaled air, as exhaled air has higher humidity. Capacitive and resistive sensors are often used for humidity measurements. Optical fibres have also been employed. Although this approach is robust against motion artefacts, it is invasive and may require the use of a face mask. Air humidity sensors have been used in ICUs.
5) Air components: measurement of level of carbon dioxide in inhaled (0.04%) and exhaled (6%) air, termed capnography, using infrared sensors and fiber optic sensors. It is an accurate technique but also intrusive due to the high number of cables and connections. Capnography enables continuous monitoring of respiratory, however usually requires use of face mask. This is the approach commonly used in ICUs.
6) Chest wall movements: respiratory monitoring based on the recording of respiratory muscles movement. Strain sensors (i.e. resistive, capacitive, inductive and fiber optic sensors) have been used for detection of chest wall movements. Additionally, transthoracic impedance sensors and movement sensors (i.e. accelerometers, gyroscopes and magnetometers) have also been deployed. Those sensors enable continuous recording of respiratory waveforms, being easily integrated into clothes and garments. This technique is unobtrusive, however, sensitive to motion artefacts.
7) Modulation cardiac activity: extraction of respiratory signal from ECG or photoplethysmography (PPG), based on the respiratory modulation of cardiac signals. The main advantage of this approach is that ECG and PPG sensors are already in use in clinical and home settings. This method is unobtrusive, but sensitive to motion artefacts.

Respiratory monitoring through non-contact methods have also been proposed [32], [43].

As the reader may notice, fiber optic sensors (FOSs) have been widely explored for respiratory monitoring purposes. Due to their good metrological properties, small size, flexibility and immunity from electromagnetic field, they are suitable to monitor patients remote and continuously, even in magnetic resonance imaging (MRI) environments, where standard electronic sensors cannot be deployed [44].

In FOSs, the optical fibre can be the sensing element (intrinsic sensors) or it can simply be used as a medium to transport light (extrinsic). There are two main types of FOSs employed in smart textiles for health monitoring: Fiber Bragg grating (FBG) technology based and intensity-based sensors [44]. Fundamentally, FBG sensors are a short segment of fiber optic, with usually 3 mm to 6 mm, which reflects a narrow range of wavelengths of the input light and transmits all the others due to exposure of the fibre core to an intense optical interference pattern. The wavelength range in which light is reflected is sensitive to temperature and strain. Thus, those sensors enable temperature and strain estimation. They have been used to monitor stroke volume, blood pressure, heartbeats as well as respiration. Similar to FBG, long period granting (LPG) sensors enable measurement of several parameters. LPG "consists of a periodic change in the refractive index profile along the fiber" [45]. Characteristics of the attenuation bands enable the measurement of strain, bending, load and temperature.

On the other hand, the working principle of intensity-based sensors is that the intensity of the light emitted by one fibre and conveyed into other fibre in close proximity to the first, is an indirect measure of the distance between the two fibres, and consequently of other parameters that influence this distance. A subtype of these group, macro-bending sensors, are based on the loss of light when the optical fibre is bent. Different bent radius result in different intensity modulations of the light transmitted by the fiber. Intensity-based sensors are used to monitor pressure and temperature. They have been proposed to measure intravascular and intracranial pressure. Macro-bending FOSs are mainly applied in respiratory movement monitoring. Table 1.2 presents some examples of sensors for respiratory monitoring based on optical fibres. Other approaches are presented in [44].

The sensor proposed by Krehel et al. [2] was developed by Empa researchers. They developed an optical fibre-based sensor that measures force or pressure applied to the sensor based on the light loss induced by changes in wave guiding properties due to changes in fibre's geometry [44].

Table 1.2. Optical fibre-based sensors for respiratory monitoring. MRI: magnetic resonance imaging.

System/ Proposition	Sensor	Working Principle	Number of sensors	Sensor Placement	Features
An Optical Fibre-Based Sensor [2]	Intensity modulated FOS	Respiratory movements	1	Torso	Non-invasive
Smart textile embedding Optical fibre sensors [46]	FBG FOS, Macro-bending FOS	Respiratory movements	2	Thorax, Abdomen	Non-invasive, MRI compatible
Respiratory Sensors Using Plastic Optical Fiber [47]	Intensity modulated FOS	Airflow, Respiratory movements	2	Nose, Abdomen	Non-invasive, MRI compatible
Respiratory function monitoring using a real-time three-dimensional fiber-optic shaping sensing scheme based upon fiber Bragg gratings [48]	FBG FOS	Respiratory movements	40	Thorax, Abdomen	Non-invasive
Respiratory monitoring using long-period fiber grating sensors [45]	LPG FOS	Bending of the chest	1	Chest	Non-invasive

Several commercially available wearable systems include sensors for respiratory monitoring. Some examples are shown in Table 1.3. The vast majority monitors breathing rate based on respiratory movements as this is the working principle more appropriate for data acquisition outside clinical setting [35].

Table 1.3. Wearable devices for remote, continuous and long-term respiratory monitoring. BR: breathing rate; TV: tidal volume, RIP: Respiratory inductive plethysmography; bpm: breaths per minute.

System	Wearable	Sensor	Working Principle	Respiratory Parameters
Equivital™ EQ02 LifeMonitor [49], [50]	Chest strap	RIP sensors	Respiratory movements	BR (0 to 70 bpm)
LifeShirt® [51]	Elastic garment (Shirt)	RIP sensors	Respiratory movements	BR, TV, minute ventilation
Zephyr™ BioHarness™ [52], [53]	Chest strap	Capacitive sensors	Respiratory movements	BR (3 to 70 bpm)
Hexoskin® [54]	Smart garment (Shirt)	Inductive sensors	Respiratory movements	BR, TV, minute ventilation
The Spire [55]	Tag	Force sensors	Respiratory movements	BR

1.2.3. Activity monitoring

In the last decades, the importance of physical activity not only for fitness but also for wellbeing and health has called the attention of health providers and scientists. Several studies show its relevance on the progress and impact of many conditions such as cancer [56], [57], cardiovascular diseases [58], pulmonary diseases, diabetes and obesity, as well as on the outcome of several medical interventions [59], [60].

The standard for physical activity and functional ability assessment in healthcare are questionnaire tools, validated functional tests, observations among other approaches. However, these methods are "either time consuming and expensive, requiring access to specialized equipment and a dedicated laboratory set-up, or they are subjective and rely on clinician observation or patient recall"[61]. Furthermore, a short-term assessment does not always reveal the condition of the patient in his/her familiar environment.

Objective measurement of subject's physical activity in home environment is possible through wearable sensors for activity monitoring. A significant part of the wearable devices for healthcare applications monitor activity. According to Mukhopadhyay [8], the most commonly used activity sensors are accelerometers, HR sensors, temperature sensors, and wearable ECG sensors. Even though gyroscopes, magnetometers, pressure sensors, microphones, and camera- and depth-based systems have also been employed [7]. Among these, accelerometers, due to their simplicity and cost-effectiveness, are the most common.

Continuous monitoring of users acceleration allows [6]–[8], [62]:

- Activity recognition;
- Classification of activity level;
- Fall prediction and detection;
- Posture recognition and analysis;
- Balance assessment;
- Metabolic expenditure estimation;
- Gait/walking patterns assessment;
- Sleep assessment.

Additionally, accelerometers are often integrated into wearable devices to use their data in algorithms for motion artifacts removal from physiological signals, such as ECG [63].

There are many wearable devices with integrated accelerometers suitable for measurements lasting several days, but there is no standard for activity monitoring in healthcare. Activity monitoring in home environment can be conducted in three modes [61]: clinical assessment, event monitoring and longitudinal monitoring.

1) Clinical assessment: Supervised, short-term monitoring. It aims to provide an objective clinical examination of the subject's particular movements, in home environment. The acquired information may be used as a complement to other physical activity and functional ability assessment approaches.

2) Event monitoring: Unsupervised and long-term monitoring; real-time data processing. It aims to accelerate the response to emergencies. Thus, this mode of monitoring requires triggering an alarm each time an abnormal event is detected (e.g. fall or absence of movement).

3) Longitudinal monitoring: Unsupervised, long-term monitoring. It aims to predict or prevent certain conditions. In this mode, parameters that quantitatively measure activity are monitored. Those parameters can be movement specific (for example step rate, postural sway and rise time) or not, which is the case for metabolic energy expenditure, amount of time spent resting and other general parameters of movement. In the first case, it is necessary to recognize the activity before measure the parameter, while in the latter there is no need for activity classification.

Wide ranges of physical activity parameters have been monitored [61]. Metabolic energy expenditure; physical activity; posture; time in activity, total sleep/awake time; walking cadence (i.e. steps/minute); variability and intensity of activity are some examples. The most common is the metabolic energy expenditure.

Although one of the main purposes of physical activity monitoring is to monitor physical activity, there is no consensus on the acceleration-derived parameters that should be used to this end. The most common parameters are step count [64]–[66] (i.e. number of steps), activity counts [67] (calculated after filtering, rectifying and aggreging acceleration over a time window [68], defined by the activity monitor manufacturer [69]), mean acceleration vector magnitude [70] (i.e. the average length of the acceleration vector) and vector magnitude units [71] (i.e. the vectorial sum of activity counts in three orthogonal directions), all calculated in 1 minute intervals. A study [72] used posture allocation to analyze sedentary behavior and inactivity.

Apart from measuring physical activity, it is important to know its distribution (at which time of day/day of the week?), frequency (how many times?), duration (time in activity) and intensity in order to analyze the activity pattern. Thus, the acquired data must have the necessary time resolution.

Some of the parameters proposed for the assessment of activity pattern based on acceleration are:

a) Gini coefficient [65], [72]: very often used for comparing patterns of accumulation (i.e. how the total value was achieved), this coefficient measures inequality among values; ranges from 0 (complete equality, i.e. all values are the same; e.g. activity bouts contribute equally to the total activity time) to 1 (complete inequality, e.g. total activity time is due to a few long activity bouts);
b) Intensity gradient [73]: measures physical activity distribution; it is the gradient of a subject's log-log linear regression which relates the activity intensity and the time accumulated at that intensity;
c) Physical activity aggregation [64]: measures activity distribution over the monitoring period, ranges from 0 (low aggregation, i.e. well spread over the monitoring period) to 1 (maximal temporal aggregation);
d) Coefficient of variation [66] : measures the variability of activity, i.e. the dispersion or spread of physical activity, $CV = 100 \times standard\ deviation/mean$;
e) Approximate entropy [66]: measures the randomness of activity fluctuations, ranges from 0 (short sequences of data points are perfectly repeatable) to 2 (any repeating sequences of points occur by chance alone);

Since there is no standard method, there is still space for new approaches to quantitatively evaluate activity patterns.

The majority of population-based studies that monitor physical activity for healthcare purposes [65], [67], [70] applied a longitudinal monitoring mode, with measurements lasting several days. The recommended duration [71] is at least 7 days to ensure the reliability of the measurement. Wearing an activity monitor can lead subjects to, intentionally or not, increase their activity level. This effect, however, tends to decrease with increasing monitoring time. Moreover, subjects' routine may greatly vary from day to day, but it is more or less constant from week to week.

Determining the "valid" monitoring period is also part of physical activity monitoring. One [64] can define the potential time of activity as the time in which the subject is awake. Thus, only data acquired while the subject was awake is taken into account in the activity pattern assessment. Others [64], [70] may consider that every time the subject can be active and so, all the data acquired while the subject wore the activity monitor is considered in the analysis. In the first case it is necessary a criterion to define sleeping periods and, in the second, a criterion must be set to determine the wearing time.

Accelerometer based physical activity monitoring is a very promising approach although it has also some limitations. One of them is that it is not suitable for monitoring activities such as resistance training, swimming or cycling. When the accelerometer is placed in central body location (e.g. waist or chest), information regarding movement of body extremities cannot be acquired. On the other side, soft tissue movement or external vibrations imposed on the body, for example while travelling in a motor vehicle, may add noise to the signal. A joint effort is needed to further explore this topic.

ActiGraph, Axivity and GENEActiv accelerometers are the ones most often used in large global surveys [73]. Several companies, such as Fitbit [74], launched smart watches with integrated accelerometers to monitor activity, recognize exercises and assess sleep quality.

1.2.4.Multi-sensor monitoring systems

The use of several wearable devices to monitor different physiological parameters is neither practical nor ergonomically sound, thus several multi-sensor systems have been proposed for continuous, long-term and remote health monitoring. However, almost none of those systems is already approved for clinical applications. Thus, they are being used for fitness or wellness purposes, while waiting for FDA and/or CE clearance. The approval of such devices will prompt advances in Telemedicine, beginning a new phase in healthcare.

VITALITI [75], develop by Cloud DX, is a wearable vital sign monitor that measures ECG, HR, oxygen saturation, respiration rate, core body temperature, blood pressure, movement, steps and posture. It enables 72 hours of continuous recording and is now undergoing FDA clearance for medical use.

Zephyr™ BioHarness™ [52], [53] is a multisensory chest strap "intended to monitor adults in the home, workplace and alternative care settings" [76]. The system monitors HR, breathing rate, activity level, subject orientation, skin temperature, blood pressure (optional external sensor) and blood oxygen saturation (optional external sensor). It has been used for sports and academics/research purposes as well as to monitor first responders (e.g. firefighters), solders and astronauts. Zephyr™ BioHarness™ is FDA-approved (510(k)). Its battery lasts 18 to 24 hours.

Hexoskin® [54] is a smart shirt that monitors ECG, breathing rate, tidal volume, minute ventilation and tri-axis acceleration-derived parameters (activity intensity, peak acceleration, steps, cadence positions and best sleep tracker). The system has 12 to more than 30 hours battery life. The battery life was increased to 48 hours with Astroskin, a system developed by the same company to monitor astronauts. Astroskin monitors blood pressure, pulse oximetry, 3-lead ECG, breathing (RIP), skin temperature, and tri-axis acceleration (activity). Both systems have been used for academic and research purposes, first responders monitoring, defense, industrial, space and aerospace applications.

Another example is EquivitalTM EQ02+ LifeMonitor [50], a device "intended for monitoring of adults (16-65 years) in hospital care facilities, the home, workplace, and alternate care settings" [76]. It is a wearable system that monitors ECG, HR, interbeat interval, respiratory rate, skin and core temperature, galvanic skin response, oxygen saturation, PPG, and activity/body position through a tri-axis accelerometer. The system has two components, the sensor electronics module and the sensor chest belt. It has FDA 510(k) clearance and is CE marked. This system was designed to provide "real-time mobile human data to keep healthy people healthy" [50]. It enables up to 48 hours of recording without recharge the battery and has been used to monitor people in extreme environments, i.e., soldiers, firefighters, athletes, miners etc.

A summary of those four systems characteristics is presented in Table 1.4. Many more wearable systems have been proposed in the literature. Even though they are not yet applied for clinical applications, they already show the great potential of wearable technology in remote, continuous and long-term monitoring of physiological signs.

Table 1.4. Multi-sensor wearable devices for remote, continuous and long-term monitoring. HR: heart rate; BR: breathing rate; TV: tidal volume.

System	Wearable	Parameters	Battery Life	Connectivity	Market Clearance
VITALITI [75]	Chest and ear device	HR, oxygen saturation, BR, core body temperature, blood pressure, acceleration	72 hours	Wireless	In process
Zephyr™ BioHarness™ [52], [53]	Chest strap	HR, BR, skin temperature, blood pressure, blood oxygen saturation, acceleration	18 to 24 hours	Wireless (Bluetooth), USB	FDA 510(k)
Hexoskin® [54]	Smart garment (Shirt)	ECG, BR, TV, minute ventilation, acceleration	12 to 48 hours	Wireless (Bluetooth)	In process
Equivital™ EQ02 LifeMonitor [49], [50]	Chest strap	ECG, HR, interbeat interval, BR, skin and core temperature, galvanic skin response, oxygen saturation, PPG, and acceleration	Up to 48 hours	Wireless (Bluetooth), SD card	FDA 510(k) and CE

This work aimed to assess the validity of the textile belt for electrocardiogram monitoring in a home setting and to supplement the existing system with sensors for respiratory monitoring. Another objective was to evaluate the suitability of the same wearable, as a multi-sensor system, for activity monitoring. The thesis is organized as follows: in Chapter 2 we assess the validity of Empa's textile belt for ECG monitoring in a home setting through a study involving patients with suspected sleep apnoea; the integration of optical fibre-based sensors into the textile belt for respiratory monitoring is discussed in Chapter 3 and, in Chapter 4, the proof of concept of an algorithm for activity monitoring using the data recorded by the textile belt (i.e. breathing rate, HR and tri-axis acceleration), as a multi-sensor system, is provided. Accelerometry-based body posture recognition is also discussed in the Chapter 4. A study was conducted to assess the validity of the textile belt for respiratory and activity monitoring. It is described in Chapter 5. Finally, the general conclusion and future prospects of the project are presented in Chapter 6.

2. ECG MONITORING

The surface ECG is a continuous record of electrical signals, generated as a response of cardiac muscles to electrical impulses generated by pacemaker cells [15]. In this way, the ECG reflects the cyclic electro-physiologic events in the myocardium, revealing the condition of heart's electrical function [16]. It has a critical role in detection of heart defects and cardiac diseases such as auricular or ventricular hypertrophy, myocardial infarction (heart attack), arrhythmias and pericarditis. ECG has also been used for emotion recognition and biometric identification [77], [78]. Figure 2.1 shows a typical ECG signal of a healthy subject.

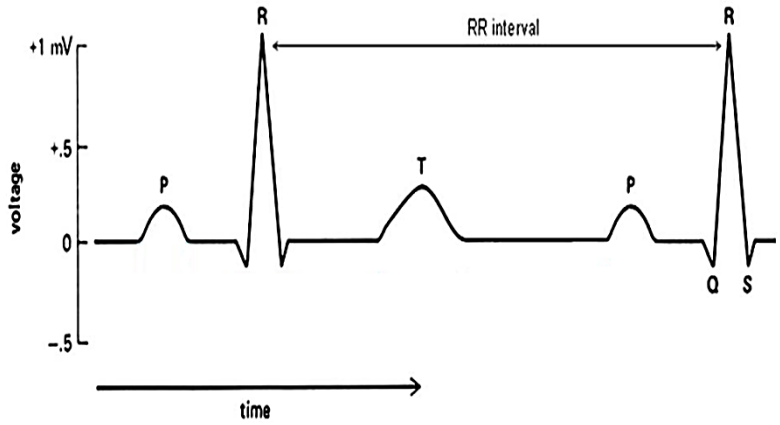

Figure 2.1. Example of ECG wave of a healthy subject. Image adapted from [79].

The ECG is characterized by its waves, segments and intervals [15]. The P wave corresponds to the atrial myocardium depolarization, the QRS complex (composed by Q, R and S waves) to the ventricular myocardium depolarization, the T wave to the ventricular myocardium repolarization and the U wave, unseen under normal conditions, in thought to be related with endocardial structures repolarization or ventricular myocardium depolarization [15], [80].

One of the most relevant ECG features is the RR-interval, the time between consecutive R peaks. It is also called heart beat interval [81]. The analysis of HRV, i.e. the fluctuations in RR-intervals, is a straightforward way to study the autonomic nervous system activity. Disease induced changes on HRV have been used for the diagnosis of several diseases, among them is sleep apnoea [82], [83].

Sleep apnoea syndrome is a disorder characterized by repetitive cessation of respiratory airflow during sleep. An apnea (Greek word which means "without breath" [84]) episode is the cessation of breathing for at least 10 seconds [85]. Apneas are classified as central or obstructive based on the absence or presence of respiratory effort (abdominal and chest wall movement), respectively. Mixed apneas are periods of absent airflow that are initially associated with an absence of respiratory effort and that persist upon resumption of respiratory effort indicating upper airway obstruction [86]. Consequently, sleep apnea is classified as central, obstructive or mixed according to the type of detected apneas. In central sleep apnea the brain fails to send the appropriate signal to the breathing muscles, resulting in cessation of the airflow. Obstructive sleep apnoea, in turn, is the obstruction of the upper airway due to pharyngeal collapse. It is more likely to occur when a supine posture is present since in this position gravitational effects are exerted on the tongue base and soft palate [87]. Partial occlusion of the upper airway is termed hypopnea. Apneas and hypopneas usually last 10 to 50 seconds, although hypopneas lasting several minutes may occur in rapid eye movement sleep [86].

Sleep apnoea syndrome severity is measured by the apnea-hypopnea index (AHI), which is the number of apneas and hypopneas per hour of sleep [4]. The gold standard for sleep apnea diagnosis is overnight PSG in a sleep laboratory. PSG incorporates recording of electroencephalogram, electro-

oculogram, chin electromyogram, snoring (microphone), oronasal airflow (thermistor), ECG, pulse oximetry and tibialis anterior electromyogram [82]. Due to the high cost of PSG and its obtrusiveness, alternative tools for sleep apnoea diagnosis have been explored. Approaches using oxygen saturation [88], snoring [89] and HRV analysis have been proposed [90].

In this context, the applicability of Empa's textile belt for overnight ECG monitoring was analyzed. A clinical study involving 242 patients with suspected sleep apnoea was carried out. Patients wore the textile belt while undergoing overnight PSG. RR-intervals derived from ECG signal recorded by the textile belt and the gel electrodes were compared. Results revealed that the belt enables RR-intervals measurement with high validity [28].

In this project, we would like to go a step further and explore the applicability of the same textile belt for ECG monitoring in home setting. No reference device was used in this study. Thus, a method to assess the quality of the acquired ECG signal, and consequently the validity of the textile belt for ECG monitoring in unattended setting, was developed. Existing approaches for ECG signal quality assessment (SQA) are described below, as well as, the method we propose.

2.1. Quality assessment of ECG signal

The frequency range of diagnostic ECG signal is 0.05 to 100 Hz [91]. Generally, when the ECG recording is clean and the heart is in sinus rhythm (i.e. electrical impulse generated by the sinoatrial node [92]), QRS complex frequency ranges between 4 and 20 Hz, and P and T waves between 0.5 and 10 Hz. Most ECG power is contained below 30 Hz [80].

Real-world ECG signals are often corrupted by various noises. Seven types of noise mainly affect ECG signals [80], [81], [93]:

a) Power line interference: noise caused by "differences in electrodes impedance and to stray currents through the patient and the cables" [94]. The noise has a frequency of 50 or 60 Hz, and an amplitude equivalent to 50% of the peak-to-peak signal amplitude. Power line noise can be modeled as sinusoids or combination of sinusoids.
b) Electrode contact noise: the loss of contact between the electrode and the skin results in abrupt baseline shifts which decays exponentially to the baseline value and has a superimposed component of 60 Hz. The noise can be permanent or intermittent and its amplitude equals the maximum recorded value.
c) Motion artefacts: changes in electrode-skin impedance caused by subject's movement result in transient baseline changes with a shape similar to one cycle of a sine wave. The baseline disturbance is of 500% of the peak-to-peak signal amplitude.
d) Muscle contraction or electromyography noise: results from the contraction of non-cardiac muscles. It can be assumed to be transient bursts of zero-mean band-limited Gaussian noise, with a standard deviation of around 10% of the peak-to-peak signal amplitude. It has a wide frequency range (DC to 10 kHz).
e) Baseline wander: baseline drift due to respiratory amplitude modulation. It can be represented as a low frequency sinusoidal wave (or combination of sinusoidal waves), of frequency between 0.15 and 0.3 Hz, and amplitude of 15% of the peak-to-peak signal amplitude. Sometimes baseline wander coincides with P and T waves frequencies.
f) Instrumentation noise: noise arising from electronic equipment used for data acquisition and signal processing.
g) Electrosurgical noise: noise of amplitude equivalent to 200% of peak-to-peak signal amplitude and frequency between 100 kHz and 1 MHz. It is produced by other medical apparatus used in parallel to ECG recordings.

Among them, power line interference and baseline wander are the most common. Although, when it comes to wearable devices, motion artefacts are predominant.

Different approaches have been proposed to assess the quality of ECG signals. In the second chapter of a recently published book [91], Orphanidou gives an overview of the existing methods for automatic assessment of ECG signal quality, especially of data recorded by wearable devices. Depending on the device application, basic quality or diagnostic quality is required. In basic quality ECG signals, R peaks are clearly identifiable; the signal enables reliable calculation of HR as well as extraction of HRV information. In ECG signals of diagnostic quality, QRS complex, P, if present, and T waves are clearly identifiable; the signal can be used for clinical diagnosis.

In summary, single- and multi-channel SQA approaches have been proposed. Some algorithms are based on time domain, while others on frequency domain features obtained from the ECG signal. The first step of SQA algorithms is beat detection. Then, feasibility checks are applied to differentiate between acceptable (i.e. high quality) and unacceptable (i.e. low quality) signal segments. Flat line detection, amplitude limits and variability, baseline wander, noise power measures and physiological feasibility have been used for SQA.

Flat signal segments are a sign of a missing lead as ECG signal is never constant. Therefore, the detection of zero or constant difference between consecutive points during a predefined time has been used for flat line recognition [95]. As mentioned before, several noises (e.g. motion artefacts, power line interference and electrode contact noise) affect signal baseline, resulting in a wide amplitude range. Thus, amplitude limits are an indicator of signal quality. Thresholds for minimum and maximum amplitude are set and, depending on the percentage of the signal outside the acceptable range, a signal segment is classified as acceptable or not [96]. Baseline wander (BLW) can be identified using a low-pass filter. A signal segment is classified as unacceptable if the BLW exceeds an empirically set threshold [97].

Noise-power measures rely on the assumption that the noise is gaussian and the signal stationary, which is not always true. Therefore, it is recommended to complement noise-power measures with other techniques that can cope with noises that do not meet these criteria. Root mean square power in the isoelectric region (i.e. region between the P wave and the QRS complex, thought to be a marker for 0 V), the ratio between in-band and out-of-band spectral power and the power in the residual after a filtering process, are some of the proposed noise-power measures [98], [99].

Lastly, signal classification using physiological feasibility relies on the well-defined range and variability of RR-intervals. The average HR (should be between 40 and 180 beats per minute), the maximum RR-interval (usually set to 1500 ms), the ratio between the maximum and the minimum RR-intervals (e.g. should not exceed 1.1 in a signal segment of 10 second as change in HR over 10% is improbable in such a short time period) have been used to reject signal segments with data that is not physiologically viable [100]. Care should be taken, however, when using physiological feasibility for SQA as it is not possible to differentiate between signal variability arising from noise and from cardiac abnormalities, such as ectopic beats (i.e. abnormal beats that are due to unusual impulses [101], they add variability to the RR-intervals).

Given that the heart follows a regular rhythm and that noise can deform ECG wave morphology, trend-based methods have been used to search for regularity in signal segments. It is assumed that the more regular an ECG segment, the higher its quality and, consequently, the more reliable is the information extracted from it. Skewness and kurtosis, which measure the symmetry and shape of a distribution, have been used to assess the regularity of ECG signal segments [102], [103]. The variability in RR-intervals, indicated for example by their standard deviation [104], and the correlation between each individual QRS complex and the reference QRS complex of the segment (often taken as the average of all QRS complexes detected in the segment), termed template matching [100], have also been used as signal quality indices.

Frequency domain approaches include analyzing the signal's frequency content in different bandwidths and spectral analysis of the HRV. Noise-power measurement methods, described previously, can be considered frequency domain methods. Those methods usually require the use of fast Fourier transform (FFT). The measurement of entropy in the different decomposition levels and other discrete wavelet transform-based methods have also been proposed for SQA [105], [106].

All signal quality indices mentioned before can be combined to provide a more robust SQA approach. Different measures have been combined through decision rules [107] or machine learning models [108]. Thresholds are applied individually to measures or classifiers, and the signal segment is classified as acceptable or not accordingly. Physiological limitations, the expected limits of signal features and empirical evidence are used to determine those thresholds. When ECG signal is acquired by multiple channels, the correlation, covariance as well as the agreement between QRS complex detected in the data from different leads have been deployed for SQA [109], [110].

We aimed to assess the quality of the ECG signal acquired in a home environment. Since the main application of the belt in the context of this study was to provide information regarding HRV for sleep apnoea detection, basic quality ECG signal is required (i.e. R peaks are clearly identifiable).

The most relevant ECG signal features are in the frequency range between 0.5 and 40 Hz [99], including the QRS complex. For this reason, ECG signals are often band-pass filtered in this frequency range [81]. Given these facts, we categorized the noises according to the frequency of their components: low-frequency, i.e. noise of frequency lower than 0.5 Hz, and high-frequency noise, i.e. noise of frequency higher than 40 Hz. BLW is a low-frequency noise, while power line interference, electrode contact noise and electrosurgical noise are considered high-frequency noise.

We used the signal-to-noise ratio (SNR), a standard measure of signal quality, to evaluate the impact of noise on the signal. The ratio between the signal power and the low-frequency noise power, referred to as SNR_{lf}, as well as between the signal power and the high-frequency noise power, referred to as SNR_{hf} were computed. Low-frequency noise was extracted from the raw ECG signal using a second-order low-pass FIR filter with cutoff frequency of 0.5 Hz, and high-frequency noise was obtained using a high-pass FIR filter of the same order, with cutoff frequency of 40 Hz. The band-pass filtered signal was taken as the reference signal. Signal's BLW was estimated based on the average amplitude of the low-frequency noise.

SNR, however, relies on the assumption that the noise follows a gaussian distribution, which is not always the case. To cope with non-gaussian and transient noises, such as motion artefacts, the physiological acceptability of the RR-intervals derived from the raw ECG signal was analyzed. This is because the presence of some noises and artefacts in the signal, e.g. motion artefacts, electrode contact noise and electrosurgical noise, lead to the appearance of peaks that can be falsely detected as R peaks. Moreover, due to BLW, T peaks can be higher than R peaks, leading to same false detection. Finally, this leads to the computation of incorrect RR-intervals. Therefore, the physiological acceptability of recorded RR-intervals is another indicator of the quality of ECG signal.

For this purpose, RR-intervals were filtered using the algorithm described by Fontana et al. [28]. RR-intervals shorter than 300 ms or longer than 1500 ms were rejected and considered as artefacts. Likewise, RR-intervals differing in more than 20% from the median of the ten preceding or following RR-intervals were excluded from further analysis as such a difference is not considered to be physiologically acceptable. The artefact percentage of each ECG recording was taken as the number of artefacts divided by the number of recorded RR-intervals. Artefact percentage was considered with respect to subjects lying position to analyze the impact of lateral pressure, which is expected to disrupt the contact between the electrodes and the skin, on signal quality.

Even though SNR_{lf}, SNR_{hf}, BLW and artefact percentage address different types of noise and enabling SQA, none of them allows differentiation between artefacts arising from noise and artefacts arising from ectopic beats. Classifying abnormal disease related events, e.g. arrhythmic events, as noise is a

common limitation of signal quality indices [111]. Differentiating between ectopic beats related and noise related artefacts is especially critical in this study as sleep apnea has been strongly associated with arrythmia [112], which increases RR-intervals variability. Therefore, we propose to apply Poincaré plots to differentiate between ectopic beats related and noise related RR-Intervals.

Poincaré plots are a quantitative and visual non-linear method to analyze HRV [15], [113]. It consists in plotting each RR-interval against the previous one. Apart from allowing the analysis of RR-intervals distribution, the visual assessment of the distribution pattern has been proved to be a tool for cardiac dysfunction prediction [114], [115], while enabling immediate recognition of ectopic beats and artefacts [115], [116]. A Poincaré plot not affected by cardiac dysfunction or noises is presented in Figure 2.2. The pattern for such a representation is called comet-shaped pattern. It reflects low variability in short-term (axis 2 direction) and high variability in long-term (axis 1 direction) while showing an asymmetry in relation to axis 2.

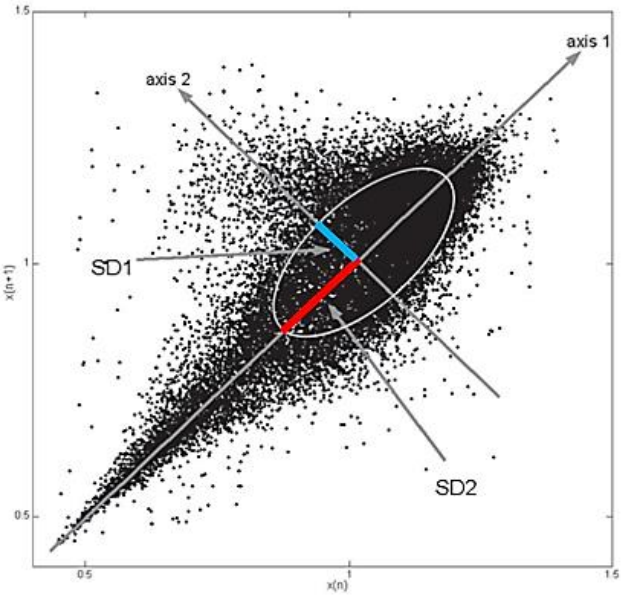

Figure 2.2. Example of Poincaré plot of a healthy subject. SD1 is the ellipse width (blue line), and SD2 the ellipse length (red line). Image adapted from [117].

Poincaré descriptors, SD1 and SD2, are used to quantitatively describe its geometry. When an ellipse is fitted to the data, as shown in Figure 2.2, SD1 corresponds to the width of the ellipse and SD2 to the length of the ellipse. The ratio between SD1 and SD2, SD1/SD2, provides an indicator for the randomness of HRV. SD1 and SD2 are calculated using equation 2.1 [118]. It has been proved that SD1 and SD2 values increase with increasing occurrence of artefacts and ectopic beats [119].

$$SD1(SD2) = \frac{1}{n}\sum_{i=1}^{n}\frac{((x_i-(+)y_i)-(\overline{x-(+)y}))^2}{2} \qquad (2.1)$$

x is the vector containing the detected RR-intervals, from the first to the penultimate; and y, the vector containing the detected RR-intervals, from the second to the last. n is the number of points in the Poincaré plot, which equals the number of detected RR-intervals minus one.

Poincaré plots showing a very low dispersion of RR-interval in the axis 2 direction are termed Torpedo-shaped; when RR-intervals are dispersed in a very symmetric way in relation to axis 2, the pattern is termed fan-shaped pattern; and when RR-interval are grouped in more than one cluster, the pattern is called complex, see Figure 2.3. The Torpedo-shaped, the fan-shaped as well as grouping in multiple

clusters are considered to be pathological [114]. Since noise is, by nature, uncorrelated and random, the presence of noise results in highly dispersed points in the plot [117]. Although Poincaré plots have been used to visually assess the quality of recorded ECG [118], the assessment of its pattern for SQA purposes has not been fully explored.

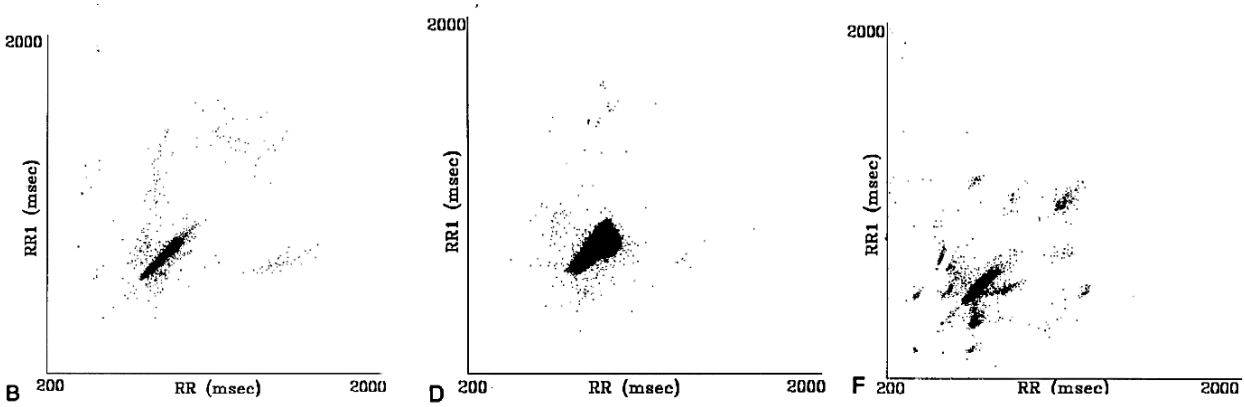

Figure 2.3. Example of pathological Poincaré plots. B: Torpedo-shaped pattern; D: Fan-shaped pattern; F: Complex pattern. Image adapted from [114].

In summary, we propose the use of SNR_{lf} and SNR_{hf} to assess the quality of the signal in terms of gaussian noise, BLW to evaluate the baseline drift, artefact percentage to measure the occurrence of artefacts due to any type of noise or physiological abnormality and, finally, Poincaré plots to determine the primary source of artefacts, i.e. ectopic beats (physiological abnormality) or noise (device malfunction).

2.2. Study: ECG monitoring in a home setting

From the 242 patients that participated in the clinical study, 12 consented to participate in this study. A description of the study participants is shown in Table 2.1.

Patients were asked to wear the textile belt for one to three consecutive nights, having received instruction on how to mount the belt during their stay in the hospital. The belt's data logger (Faros 180◦, Bittum Corporation, Oulu, Finland) was activated by study nurses, consequently, subjects' ECG signal was continuously recorded during the whole period of participation in the study.

Table 2.1. Description of study participants. Comparison with the clinical study. BMI: body mass index. AHI: apnea-hypopnea index.

		Full data set of the clinical study	Subgroup of this study
n		242	12
Age (y)		52 [43-61]	54 [48-59]
male/female		186 / 56	10 / 2
BMI ($kg \cdot m^{-2}$)		29 [25.5-32.5]	30.0 [28.0 – 35.5]
AHI (h^{-1})		21 [4.4 – 37.6]	14.8 [8.6 – 38.5]
Type of apnoea	Obstructive	156	8
	Central	5	1
	Mixed	35	1
	Unspecified	1	0
	No apnoea detected	44	2

Selection of valid monitoring periods

After completion of data collection, a single ECG recording was obtained for each patient. Thus, monitoring periods, i.e. nights, had to be selected from the recordings. The first and last point of monitoring periods were determined manually. Since patients were instructed to only wear the belt when going to sleep, the starting point of a valid monitoring period was considered to be the "first ECG signal segment clear enough to be recognized as such, after several hours without any recorded ECG signal" [27]. Likewise, "the end of each monitoring period was defined as the last ECG signal recorded before a long period of signal absence." [27]. Data recorded by an acceleration module integrated in the ECG data logger was considered for the confirmation of selected monitoring periods. ECG data was recorded with a sampling frequency of 250 Hz, and tri-axis acceleration with a sampling frequency of 10 Hz. Acceleration data was also used to recognize subjects' lying position.

Signal processing and data analysis

R peaks were detected using Kubios HRV Premium Software, Version 2.2 (Kubios Oy, Kuopios, Finland). RR-intervals were computed by the same software. Signal processing algorithms were implemented in MATLAB R2018a (The MathWorks, Inc., Natick, MA, USA). All statistical analysis was carried out using R, version 3.4.3 (R Foundation for Statistical Computing, Vienna, Austria). The author used Microsoft Excel (Microsoft Corp., Redmond, Washington, USA) for calculations. A p value of less than 0.05 was accepted as the level of statistical significance. Hereafter, data is presented as average value ± standard deviation.

2.2.1 Results and discussion

A total of 28 valid monitoring periods (i.e. nights) were identified, three nights in seven patients, two nights in two patients, and one night in three patients. The average duration of nights was 7.7 ± 1.2 h. The quality of the data acquired by the textile belt in the home setting (ECG-belt home) was assessed and compared to the quality of the data acquired by the gel electrodes (Gel electrodes) and the textile belt (ECG-belt hospital) during the clinical study.

The ECG signal acquired in the home setting had a good quality (Table 2.2). SNR_{lf} and SNR_{hf} were found to be high showing values similar to those of the data acquired by the gel electrodes in clinical

setting. Likewise, BLW of the ECG signals acquired by the belt in home environment is much lower than the one of the data acquired by the same device in the hospital, being close to the BLW of the data acquired by the gel electrodes. A great improvement was noticed on the data quality acquired by the textile belt when compared to the clinical study data, especially in terms of low-frequency noise.

Table 2.2. Comparison of the quality of ECG signals recorded in the hospital (Gel electrodes and ECG-belt hospital) and at home (ECG-belt home).

	SNR_{lf}	**SNR_{hf}**	**BLW**
Unit	dB	dB	mV
Gel electrodes	12 ± 5	21 ± 3	0.03 ± 0.02
ECG-belt hospital	0 ± 5	17 ± 6	0.30 ± 0.43
ECG-belt home	11 ± 2	21 ± 5	0.05 ± 0.02

In average, 7.49% of the RR-interval derived from the ECG signals acquired by the belt were considered as artefacts. Even though the artefact percentage was lower than the one of the data acquired in clinical environment, it was still higher than the one of the gel electrodes, see Table 2.3.

Table 2.3. Artefact percentage of RR-intervals derived from the ECG recordings. Data of the gel electrodes (Gel electrodes) and the ECG-belt (ECG-belt hospital) in hospital and of the ECG-belt in home environment (ECG-belt home).

	Gel Electrodes	**ECG-belt hospital**	**ECG-belt home**	**N**
Average	2.87%	9.66%	7.49%	12
Median	1.41%	5.38%	2.77%	
SD	4.14%	14.65%	10.76%	

Poincaré plots revealed to be effective for determining the primary source of artefacts, whether ectopic beats or noise (Figure 2.4).

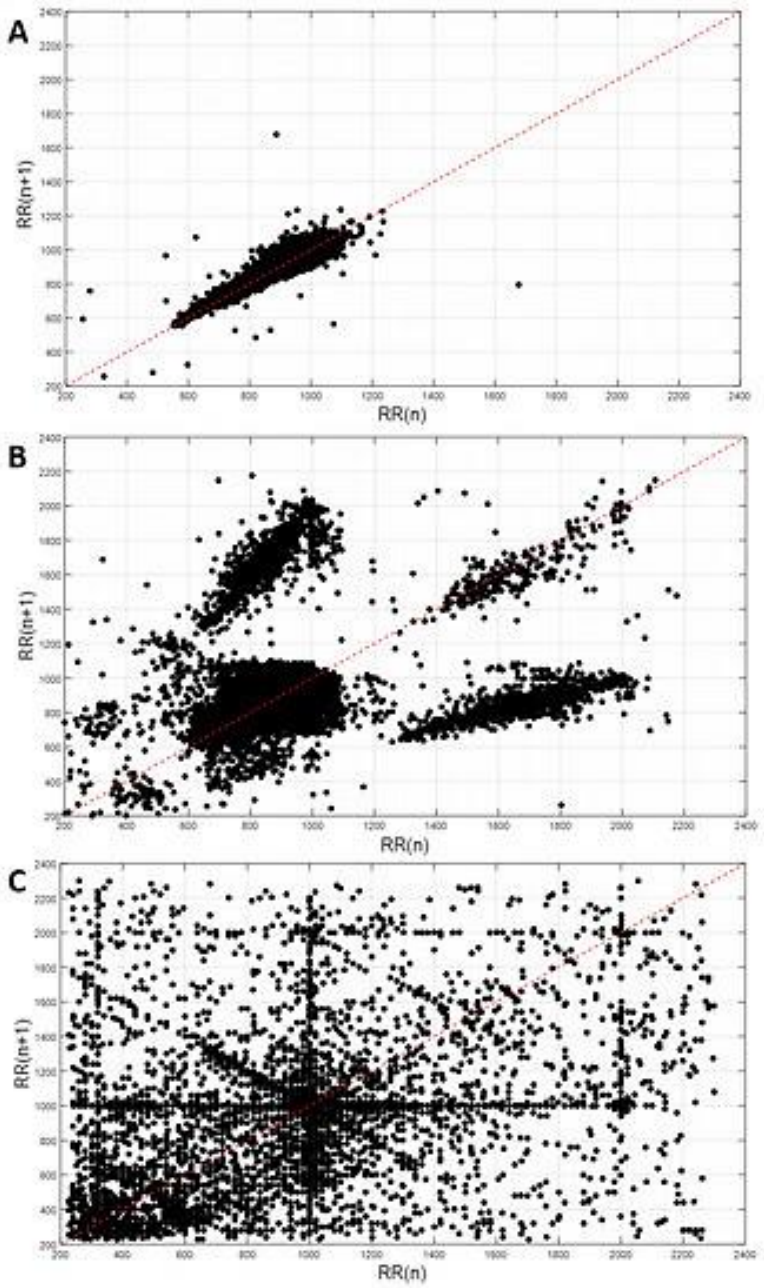

Figure 2.4. Example of Poincaré plot. A: artefact percentage of 0.2%; B: artefact percentage of 6.2%, artefacts caused by pathophysiological issues; C: artefact percentage of 11.3%, artefacts caused by noise. Unfiltered RR-intervals. Image and caption taken from [27].

While in A the low artefact percentage indicates a good ECG signal quality, in C ECG signal was corrupted by power line noise, resulting in a high artefact percentage and a consequent highly scattered points distribution [117]. In B, the artefact percentage is also high, i.e., higher than 5%. However, Poincaré plot distribution shows a complex pattern, indicator of heart disease [120]. Thus, artefacts do not arise from low quality ECG signal, but are characteristic of the subject. Interestingly, a similar complex pattern was also found for data of the same subject acquired in other two nights (see Figure A11 in Appendix A). The suspect of cardiac disease was confirmed, proving once again the potential of Poincaré plots for HRV analysis. In line with other works, Poincaré plot descriptors were found to be significantly correlated with artefact percentage, especially SD1 (see Table 2.4).

Table 2.4. Correlation between artefact percentage and Poincaré plot descriptors (SD1, SD2 and SD1/SD2). Filtered RR-intervals; patient with cardiac disease was excluded.

	Correlation	*p*
SD1	0.80	< 0.001
SD2	0.47	0.02
SD1/SD2	0.62	< 0.001

We found that an artefact percentage of 3% or lower was associated with a very clean Poincaré plot, i.e. clear pattern with almost no artefacts due to ectopic beats nor noise. Interestingly enough, the average artefact percentage of the data acquired by the gel electrodes during the clinical study was 2.87%, which corroborates our finding. Artefact percentages equal or lower than 3% were found for 15 of the 28 nights (53.6%). Furthermore, 4 of the 13 nights with artefact percentage higher than 3% had ectopic beats as the primary source of artefacts (see Figures A10 and A11 in Appendix A). Thus, the data acquired by the textile belt was found to be of low quality only in 9 of the 28 nights (32.1%). Poincaré plots also showed that the RR-intervals filtering algorithm greatly improved the quality of RR-intervals data (see Poincaré plots in Appendix A).

Even though the textile belt is more sensitive to noise than the gold standard (i.e. its data has a higher artefact percentage), a mean difference of -32.69 ms was found between the average RR-interval of the data acquired in the home setting and the data acquired by the gel electrodes in clinical setting. The mean difference increases to -42.45 ms when compared to data recorded by the textile belt in clinical setting. Given that home measurements were conducted on different nights in a different environment, this difference can be considered as acceptable. Besides, average RR-intervals measured in the different settings were found to be highly correlated (Pearson r of 0.78, $p = 0.003$). It shows good agreement between RR-intervals derived from the ECG recordings in home and clinical settings.

Finally, Figure 2.5 shows the artefact percentage according to subjects lying position. Data was considered for analysis only when recordings for subjects remaining more than 1 minute in the same position were obtained. In accordance with the conclusions of the clinical study, lying in a lateral position is associated with increased artefact percentage. It is thought to be caused by loss of contact between electrodes and the skin due to belt deformation induced by lateral pressure.

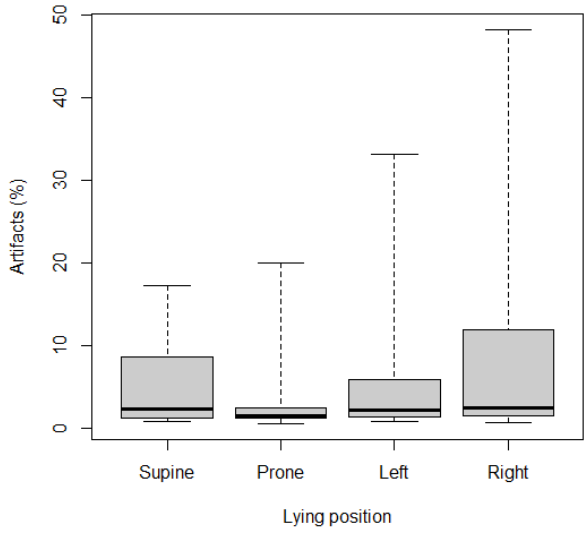

Figure 2.5. Boxplot of artefact percentage according to subjects lying position. Black line indicates the median; gray area indicates the interquartile range. Whiskers extended from minimum to maximal values.

The results of the SQA of the ECG signal acquired by the textile belt in the home setting were published by Fontana et al. [27] including further discussions of the results.

2.2.2 Conclusions

Our results revealed that ECG signals acquired by the textile belt in the home setting achieved better quality than the data acquired by the same device in clinical setting. It has a higher SNR, actually similar to the one of ECG signals acquired by the gel electrodes, and a lower artefact percentage. Even though the data recorded in the home setting has a higher artefact percentage than the data acquired by the gel electrodes, a good agreement was found between the RR-intervals derived from ECG recorded in the two settings.

Poincaré plot analysis showed the suitability of the textile belt to record reliable ECG signals, even in a home environment. Visual assessment of Poincaré plots proved to be effective for the determination of the primary source of artefacts (noise or ectopic beats). The development of an algorithm for automatic recognition of Poincaré plot pattern would be of great value, as the need of human intervention is the main limitation of this technique.

It is unclear why data recorded in the home setting is of higher quality than the data obtained in clinical setting. As a low number of patients were included in this study (pilot study), a follow-up study and further research is needed. In this study no information regarding the way patients handled the belt neither regarding possible 'artefacts sources' present in the monitoring environment was available. A deeper analysis must be conducted in order to better understand the behavior of the belt, especially the possible sources of artefacts and their effect on signal quality (e.g. wear the belt in a wrong way, presence of electronic devices near the belt, etc.). Such a study must be conducted in a controlled environment. The effect of body posture was analyzed; however, it would also be interesting to analyze the effect of movement due to posture transitions on signal quality.

The use of the textile belt in a home setting enables continuous, remote and non-invasive ECG monitoring, while ensuring patients' comfort. It would be valuable not only for the pre-screening of patients with suspected sleep apnoea, but also for long-term monitoring of patients suffering from sleep apnoea and other sleep-related disorders that affect HRV as well as the observation of treatment efficacy [27].

3. RESPIRATORY MONITORING

---------- Content Removed ----------

4. ACTIVITY MONITORING

In recent years, the importance of physical activity for both physical and mental health has been proved. Physical inactivity was pointed as the fourth leading risk factor for mortality, following high blood pressure, tobacco use and high blood glucose [121]. Several studies have highlighted the crucial role of physical activity in the reduction of risk for cardiovascular diseases [122]–[124] and cancer mortality [125], [126], as well as for the improvement of mental health [127], [128]. Furthermore, physical activity improves the quality of life of patients suffering from different diseases, for example fibromyalgia [129] and autoimmune diseases [130], and reduction in activity level is an early sign of Parkinson disease [131]. As a result, an effort to increase public awareness on the risk of a sedentary lifestyle has been done. Activity monitors play a major role in achieving this purpose.

A brief discussion on the relevance of physical activity intensity and body posture recognition for activity monitoring is presented in this chapter. Algorithms for determining activity intensity and recognizing body posture based on the data from the acceleration module integrated in the ECG-belt logger are proposed here.

4.1. Physical Activity Intensity

Given the strong scientific evidences of the benefits of an active lifestyle, in 2010 the WHO launched the Global Recommendations on Physical Activity for Health [121]. It aimed to prevent non-communicable diseases (often called chronic diseases), the leading cause of death worldwide [132], through physical activity at population level. In this book, the WHO addresses the recommended level of physical activity for adults and children aged 5 years and older. As an example, recommendations for adults aged between 18 and 64 years, are the following**:**

1. Adults aged 18–64 should do at least 150 minutes of moderate-intensity aerobic physical activity throughout the week, or do at least 75 minutes of vigorous-intensity aerobic physical activity throughout the week, or an equivalent combination of moderate- and vigorous-intensity activity.
2. Aerobic activity should be performed in bouts of at least 10 minutes duration.
3. For additional health benefits, adults should increase their moderate-intensity aerobic physical activity to 300 minutes per week, or engage in 150 minutes of vigorous-intensity aerobic physical activity per week, or an equivalent combination of moderate- and vigorous-intensity activity.
4. Muscle-strengthening activities should be done involving major muscle groups on 2 or more days a week. [121, p8]

These recommendations show that a comprehensive description of physical activity, it is important to get information about the duration (“For how long”), frequency (“How often”), intensity (“How hard a person works to do the activity”) and volume (“How much in total”) [121]. Therefore, any device intended to monitor physical activity for healthcare purposes must be able to provide this information. Activity duration, frequency and volume, as well as information regarding activity distribution, i.e. time of the day/day of the week, simply rely on the acquisition of data with the necessary time resolution. However, determining physical activity intensity implies the knowledge of the activity specific energy expenditure.

In [133], [134], the different techniques to measure energy expenditure (EE) are presented. Self-reporting methods were one of the first approaches used to assess physical activity and are still widely used in clinical practice. Nevertheless, self-reporting methods rely on subjects’ memory and perception [135], [136]. Thus, in spite of their low cost, these methods have low reliability and accuracy when assessing physical activity EE [137].

The gold standard for measuring total energy expenditure (TEE) is the doubly labeled water (DLW). It consists on the ingestion of a known dose of $^{2}H_{2}{}^{18}O$ and $^{2}H_{2}{}^{16}O$ and calculation of the TEE based on the difference between the elimination rates of the two isotopes. Elimination rates are determined through analysis of urine, saliva or blood samples, collected at different times during the measurement period, by mass spectroscopy [138]. DLW enables measuring the average daily TEE under free-living conditions with high accuracy and is non-invasive. Despite that, it is expensive, requires qualified personnel and implies samples collection.

Other popular techniques for EE measurement are the direct and the indirect calorimetry. The direct calorimetry enables the determination of subjects' metabolic rate based on the measurement of their rate of heat loss using a calorimeter. Subjects must be in an insulated chamber during the measurement. It is the most accurate method to measure metabolic rate but is also costly and a burden for participants. The indirect calorimetry is the most commonly used technique to measure EE. It is an accurate and non-invasive method. Weir's formula is used to calculate EE based on the volume of consumed O_2 and produced CO_2, quantified through the measurement of the concentration of the two gases as well as the inspired and expired volumes of both. Douglas bag, canopy or facemask are used to measure gas concentration and volume, which makes the procedure impractical, especially in free-living environment.

EE can also be estimated based on physiological variables such as HR [139]–[141], core temperature [142] and pulmonary ventilation volume [143], [144]. It is known that HR is linearly related within a particular range of EE [145], thus the later can be indirectly measured after finding the linear function that describes this relation [145], [146]. Apart of being non-invasive, it is more affordable than the other methods and allows free-living measurement of EE using HR monitors. This method has, however, two main limitations: the linear relationship between EE and HR varies from subject to subject and it deteriorates at sedentary and very intense activities [145]. Despite these limitations, the level of physical activity has been determined based on the HR [147], [148].

Additionally, motion sensors, such as accelerometers and pedometers have been used to estimate EE. Pedometers measure the number of steps a person takes in a certain time interval. They are low cost and unobtrusive, yet inaccurate for EE estimation. Even so, the number of steps per minute (cadence) has been used to determine physical activity intensity [149]–[151]. Accelerometers measure the acceleration exerted upon the sensor with reference to the gravitational force, g ($g = 9.81\ m/s^2$), in one to three orthogonal directions [133], [152]. They enable long-term activity monitoring in free-living populations and provide information regarding the volume, frequency, intensity and duration of physical activity [153]. Prediction models have been developed to estimate EE based on acceleration derived parameters, though their application is limited [134], [154]. Accelerometer based EE estimation is a low cost, reliable, objective and practical method, however studies revealed that the estimation accuracy is low for sedentary-to-light activities [155] and that the linear relation between acceleration and EE depends on the type of activity performed [156], [157].

The most frequently used reference measure of activity intensity is the metabolic equivalent of the task (MET) which is expressed as energy expended per body mass and time (1 MET = 1 kcal/(kg body mass.h)) or as metabolic power per body surface area (1 MET = 58.2 W/m^2). 1 MET represents the resting metabolic rate, defined as the energy cost of sitting quietly [158]. Activity intensity is usually divided in three levels: light (<3METs), moderate (3-6 METs) and vigorous (>6 METs) [131], [147], [149], [154].

The WHO considers moderate-intensity physical to increase HR above resting HR and vigorous-intensity physical to substantially increase HR and cause rapid breathing [158]. Given that Empa's textile belt enables HR and breathing rate (BR) monitoring, and has an acceleration module integrated in the ECG logger, the use of all these parameters to determine physical activity intensity was explored.

4.1.1. Algorithm for physical activity intensity classification

As mentioned above, HR has been used to determine physical activity intensity. It is done by calculating the percentage of the maximal HR (HR_{max}), called $\%HR_{max}$. American College of Sports Medicine (ACSM) guidelines [147] define light-intensity activities as requiring more than 50% HR_{max}, moderate-intensity as requiring more than 64% HR_{max} and vigorous-intensity as requiring more than 77% HR_{max}. The HR_{max} is often taken as the age-predicted HR_{max}, calculated using the formula HR_{max} = 220-age [135].

In [148], light-intensity activity is associated with a slight increase in BR, moderate-intensity with a more notable increase in BR and vigorous-intensity with being more out of breath. In contrast with the HR or the oxygen uptake, so far, the BR has not been considered to assess physical activity intensity. However, recently a paper entitled "Respiratory Frequency During Exercise: The Neglected Physiological Measure" [159] aimed to put the attention to the relevance of BR as a marker of physical effort. Nicolò and co-authors listed several advantages of considering BR for training monitoring based on the existing scientific evidence. BR response to incremental exercise is approximately linear; BR time course has been proved to be related with that of Rating of Perceived Exertion (RPE), which is a subjective measure of physical activity intensity; and BR may be an indicator of time to exhaustion. Most interestingly, and in contrast with HR and other physiological parameters, BR responds very fast to changes in effort which occur due to workload variations. Moreover, the relation between BR and physical effort does not depend on the active muscle mass nor on the metabolic requirements of the activity. In their paper, Nicolò and colleagues suggest methodologies on how to analyze BR data. They propose the normalization of BR by relating it to the maximal BR (BR_{max}), in a similar way as $\%HR_{max}$. This would handle the great variability of the BR and therefore facilitate data analysis and generalization of conclusions. Yet, it implies conducting tests to measure BR_{max} or take the maximum BR recorded during the monitoring period as the BR_{max}. A first study analyzed the suitability of BR normalized to BR_{max} for the assessment of physical activity effort. Their findings revealed a high correlation between the percent of BR_{max} and RPE [160].

We propose the use of the ratio between the BR and the resting BR (BR_{rest}) as an indicator of physical activity intensity. Even though it does not have a well-defined range of variation as the percentage of BR_{max}, it is easier to measure BR_{rest} than BR_{max}. Thus, normalization of BR to BR_{rest}, through the formula BR/ BR_{rest}, may be another way to normalize BR.

As the HR, accelerometry has been commonly used for physical activity intensity classification. In fact, accelerometers are the sensors most commonly used for activity monitoring, of which ActiGraph accelerometers are the most popular. Since the output of ActiGraph accelerometers was not the raw acceleration (available for newer ActiGraph accelerometers) but counts per unit time, counts is the most used metric of physical activity [68]. Consequently, activity intensity has been widely determined based on the number of counts per minute [67], [129], [161]. Nevertheless, since the definition of activity count varies among devices, the use of raw acceleration data has been advised to ensure comparability between studies. In this way, several studies [73], [162], [163] classified activity intensity based on cut points for the average acceleration, usually presented in milligravity (mg).

Though accelerometry is an objective method to measure physical activity, the same activity may require different effort for different subjects since the intensity of physical activity also depends on subject's fitness, age and gender, for example. Besides, in the system proposed in this work, the accelerometer is placed in the anterior chest. It is a good position to record motions that involve displacement of the entire body, yet information regarding movement of body extremities cannot be acquired and activities such as resistance training, swimming or cycling cannot be adequately recorded [156], [157]. On the other hand, HR and BR vary with physical activity, regardless of the activity type, and reflect individual characteristics. However, both change as a body response to emotional,

physiological and environmental factors [164]. Therefore, combining HR, BR and acceleration is a sound manner to overcome the limitations of each parameter.

The combination of HR and acceleration to estimate EE has been widely explored, and results proved that it improves estimation accuracy when compared to models using HR or acceleration only [165]–[167]. In [168], a wearable device that monitors HR through electrocardiography, relative tidal volume through impedance pneumography and acceleration from upper and lower limbs is presented. A multilayer perceptron neural network model for EE estimation was developed. The model includes $\%HR_{max}$, normalized relative ventilation (i.e. ratio between the sum of the relative tidal volumes measured in a short time interval and the maximal relative ventilation) and mean absolute value of wrist and thigh acceleration as input features. Results show a good agreement between model estimates and reference methods. Preliminary tests of another wearable system for activity monitoring is presented in [169]. This wearable device monitors BR, HR and movement cadence by a variable-orifice meter combined with a differential pressure sensor, a photoplethysmographic sensor and an IMU unit, respectively, in real time. Even though the system was designed for activity monitoring, methods for the use of the measured parameters for this purpose were not explored. In [170], EE was estimated based on different parameters such as acceleration (activity, acceleration peaks count), HR, BR, chest skin temperature, galvanic skin response, arm skin temperature and ambient temperature. Different regression models were applied for the different parameters and combined the outputs by calculating the median. The combination of the different models resulted in a lower mean absolute percentage error.

The proof of concept for activity intensity classification based on the combination of HR, BR and acceleration monitored by the textile belt was developed. The acceleration module of the belt's data logger records acceleration in three orthogonal axes. After data acquisition, the raw data is filtered using a third-order elliptical filter (cutoff frequency: 0.3 Hz, passband ripple: 0.1 dB, stopband: −100 dB) [171] in order to separate inertial acceleration (*ic*), associated with body movement, from gravitational acceleration, which is related with body posture. For each axis, *ic* was integrated by calculating the Euclidean norm. The inertial acceleration magnitude is given by

$$ic = \sqrt{{ic_x}^2 + {ic_y}^2 + {ic_z}^2} \tag{4.1}$$

The inertial acceleration magnitude is, afterwards, averaged in 30-second epochs, without overlapping. BR and HR are averaged in the same manner. HR is derived from the measured RR-intervals, according to the formula

$$HR = \frac{60}{RR} \tag{4.2}$$

where *RR* is the RR-interval (in seconds) calculated from the ECG signal.

The algorithm for activity intensity classification consists of finding the discriminants that enable correct classification of activities as light, moderate or vigorous, based on single parameters, and combining classifications using four rules. The discriminants for HR [147] and acceleration [70], [73], [158] were determined based on the available literature, while the discriminants for the BR were empirically determined. All thresholds are presented in table 4.1.

Table 4.1. Discriminants for activity intensity classification.

	Discriminants	
	Moderate	Vigorous
$\%HR_{max}$	64%	77%
Ratio BR_{rest}	1.5	2
ic	80 mg	500 mg

Depending on the parameters value of a given 30-second epoch, the activity performed by the subject is classified as light, if the value is less than the cut point for moderate-intensity activity; moderate, if the value is equal or higher than the moderate-intensity cut point; and vigorous, if it is equal or higher than the vigorous-intensity cut point.

The different classifications, based on HR (cHR), BR (cBR) and inertial acceleration (cIc) are combined using four basic rules:

1) If the average acceleration over a certain epoch was lower than 20 mg, the epoch is classified as inactive, and no activity level is assigned to that epoch;
2) If cHR, cBR, and cIc are equal, the level of activity is the one indicated by all parameters;
3) If cIc indicates moderate-intensity activity and cHR vigorous-intensity activity, the activity intensity is classified as moderate;
4) If each parameter points to a different activity intensity, the physical activity intensity is the one closest to the mean classification.

The first rule ensures the distinction between active and inactive periods and the third is intended to cope with activities that cannot be fully recorded by the accelerometer. In order to calculate a mean classification, a numerical index was assigned to each activity level: -1 to inactivity, 0 to light, 1 to moderate and 2 to vigorous-intensity physical activity. The flow chart of the proposed algorithm is provided in Figure 4.1.

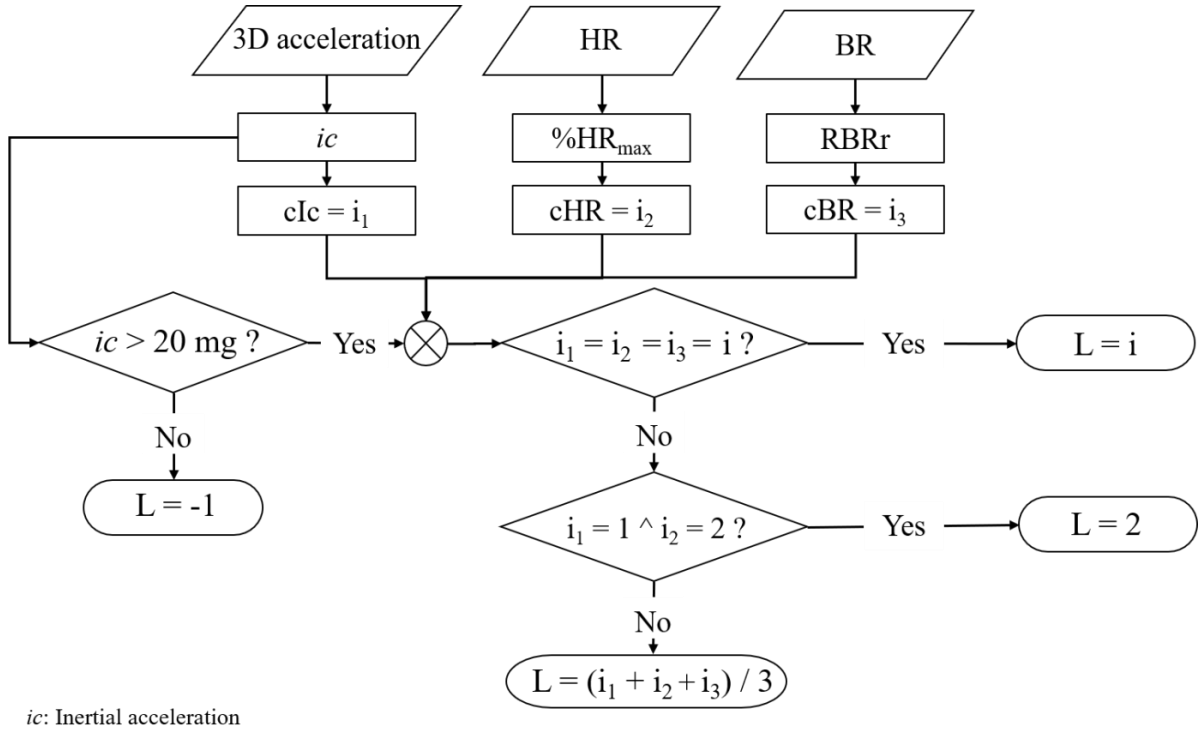

ic: Inertial acceleration
$\%HR_{max}$: percentage of maximal HR
RBRr: ratio between the BR and the resting BR
cHR: classification based on HR
cBR: classification based on BR
cIc: classification based on *ic*
L = activity intensity | -1: Inactivity; 0: Light-intensity activity; 1: Moderate-intensity activity; 2: Vigorous-intensity activity

Figure 4.1. Flow chart of the algorithm for activity intensity classification.

4.2. Algorithm for body posture recognition

Another important aspect besides activity monitoring is body posture recognition, particularly for general activity assessment and during sleep. Subjects' sleep position has been proved to have a relevant role in many diseases, such as benign paroxysmal positional vertigo [172] and sleep apnea [173], [174]. In fact, body position is one of the parameters monitored during PSG, the standard method for the diagnosis of sleep-related breathing disorders [174]. Furthermore, body posture is strongly associated with sedentary behavior, being a good indicator of how active individuals are [72].

Accelerometry has been widely used for body posture recognition [175], [176]. The most important features for posture recognition based on acceleration are the orientation angles, i.e. the angles between the gravity vector and angles of the axes [177]. For example, tilt angle, i.e. the angle between the gravity vector and the z axis, is a relevant feature for activity recognition [178] and trunk inclination, i.e. the angle between the gravity vector and the x axis, has been used to differentiate lying, sitting and standing postures for sensors applied on the trunk [177]. Waist and thigh angles have also been used for posture recognition [179]. Apart from the sensor placement, a crucial issue when recognizing body posture through the use of orientation angles is to determine threshold limits, i.e. the tolerance angles, for each position to be identified [180]. A tolerance angle of 45° has been widely used [176], [179], [180] since it allows uniform distribution of body postures in terms of angular range.

We developed an algorithm for lying position recognition based on the data recorded by the textile belt accelerometer. When subjects wear the textile belt, accelerometer's x-axis points to subjects' vertical direction, y-axis to the mediolateral and z-axis to the anteroposterior direction, see Figure 4.2. Therefore, the algorithm calculates the angle between the gravitational acceleration projection onto the

yz plane (transverse plane) and the y (β) and z (γ) axes (see equation 4.3) to determine subjects' lying position (supine, prone, left or right).

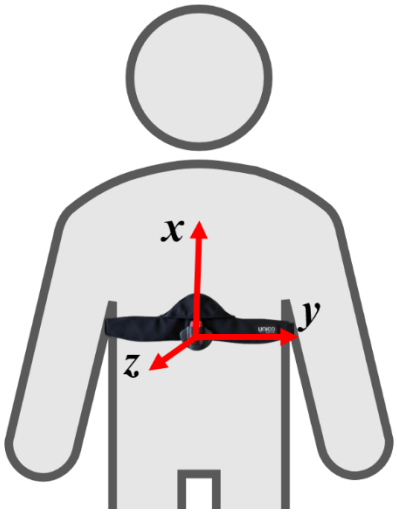

Figure 4.2. Axes directions of the accelerometer integrated in belt's data logger.

When the gravitational acceleration magnitude in the y (g_y) and z (g_z) axes are lower than 700 mg, the body posture is identified as not lying, i.e. standing or sitting. A tolerance angle of 45° is used for all positions. In order to increase the algorithm performance, the use of the inclination angles in the mediolateral and anteroposterior directions, i.e. the angle between the gravity vector and the y (*taY*) and z (*taZ*) axes (equation 4.4), respectively, was investigated. For posture recognition, only the gravitational acceleration is considered. For this purpose, the recorded acceleration is filtered using the elliptical filter described in the previous section.

$$\beta\ (\gamma) = \frac{g_{y(z)}}{\sqrt{{g_y}^2+{g_z}^2}} \tag{4.3}$$

$$taY\ (taZ) = cos^{-1}(g_{y(z)}) \tag{4.4}$$

A preliminary study was conducted to test the appropriateness of the textile belt for activity monitoring based on the algorithms discussed here. The study is described in the following chapter.

5. VALIDATION STUDY

--- Content Removed ---

6. CONCLUSION AND FUTURE WORK

This thesis aimed to explore the use of a textile belt developed by Empa as a multi-sensor wearable system for long-term, remote and continuous ECG, respiratory and activity monitoring. The textile belt consists of a chest strap with two embroidered textile electrodes and an integrated reservoir that releases water vapor to moisturize the electrodes. The signals acquired by the textile electrodes are stored in a data logger.

A study involving patients with suspected sleep apnoea was conducted to explore the suitability of the textile belt for ECG monitoring in a home setting. Signal-to-noise ratio, baseline wander, artefact percentage and Poincaré plots were used to assess the quality of acquired signals. This signal quality assessment approach was found to be effective. Results revealed that the textile belt can acquire 1-lead ECG signals of good quality in a home setting. A good agreement was found between the RR-intervals derived from ECG recorded in home and clinical settings.

Data from the acceleration module integrated in the belt's data logger was used for posture recognition based on orientation angles. Our method achieved the accuracy required for such applications. Additionally, the proof of concept of an algorithm for physical activity intensity classification based on inertial acceleration, heart rate and breathing rate was presented. Preliminary results yielded high accuracy, showing the potential of combining those three parameters for activity monitoring.

Additional pilot and clinical studies have to be conducted to corroborate our findings and further prove the clinical relevance of data acquired by the textile belt. The use of the textile belt for sleep assessment based on accelerometry, or apnoea detection using the signal acquired by the optical fibre-based sensors, would ensure maximal use of the data recorded by this system.

The current thesis supports the need for multi-sensor wearable devices for healthcare applications. The integration of sensors into a textile belt proved to be appropriate for long-term, remote and continuous monitoring of subjects' physical and physiological parameters, having the potential to be used as tool for disease prediction and diagnose support.

REFERENCES

[1] M. Weder *et al.*, "Embroidered Electrode with Silver/Titanium Coating for Long-Term ECG Monitoring," *Sensors*, vol. 15, no. 1, pp. 1750–1759, Jan. 2015.

[2] M. Krehel, M. Schmid, R. Rossi, L. Boesel, G.-L. Bona, and L. Scherer, "An Optical Fibre-Based Sensor for Respiratory Monitoring," *Sensors*, vol. 14, no. 7, pp. 13088–13101, Jul. 2014.

[3] A. Aliverti, "Wearable technology: role in respiratory health and disease," *Breathe*, vol. 13, no. 2, pp. e27–e36, Jun. 2017.

[4] S. Fuhrhop, S. Lamparth, M. Kirst, G. V. Wagner, and J. Ottenbacher, "Ambulant ECG Recording with Wet and Dry Electrodes: A Direct Comparison of two Systems," in *IFMBE Proceedings*, vol. 25, no. 5, 2009, pp. 305–307.

[5] P. Verdecchia *et al.*, "White coat hypertension and white coat effect similarities and differences*," *Am. J. Hypertens.*, vol. 8, no. 8, pp. 790–798, Aug. 1995.

[6] S. Majumder, T. Mondal, and M. Deen, "Wearable Sensors for Remote Health Monitoring," *Sensors*, vol. 17, no. 12, p. 130, Jan. 2017.

[7] M. Cornacchia, K. Ozcan, Y. Zheng, and S. Velipasalar, "A Survey on Activity Detection and Classification Using Wearable Sensors," *IEEE Sens. J.*, vol. 17, no. 2, pp. 386–403, Jan. 2017.

[8] S. C. Mukhopadhyay, "Wearable Sensors for Human Activity Monitoring: A Review," *IEEE Sens. J.*, vol. 15, no. 3, pp. 1321–1330, Mar. 2015.

[9] O. D. Lara and M. A. Labrador, "A Survey on Human Activity Recognition using Wearable Sensors," *IEEE Commun. Surv. Tutorials*, vol. 15, no. 3, pp. 1192–1209, 2013.

[10] D. Dias and J. Paulo Silva Cunha, "Wearable Health Devices—Vital Sign Monitoring, Systems and Technologies," *Sensors*, vol. 18, no. 8, p. 2414, Jul. 2018.

[11] Y. Athavale and S. Krishnan, "Biosignal monitoring using wearables: Observations and opportunities," *Biomed. Signal Process. Control*, vol. 38, pp. 22–33, Sep. 2017.

[12] European Parliament and the Council of the European Union, "Regulation (EU) 2017/745 of the European Parliament and of the Council of 5 April 2017 on medical devices, amending Directive 2001/83/EC, Regulation (EC) No 178/2002 and Regulation (EC) No 1223/2009 and repealing Council Directives 90/385/EEC and 93/42/EE," *Official Journal of the European Union*, 2017. [Online]. Available: https://eur-lex.europa.eu/legal-content/EN/TXT/?uri=CELEX%3A32017R0745. [Accessed: 17-Sep-2019].

[13] Food and Drug Administration, "Is The Product A Medical Device? | FDA," 2018. [Online]. Available: https://www.fda.gov/medical-devices/classify-your-medical-device/product-medical-device. [Accessed: 17-Sep-2019].

[14] James Hayward, "Wearable Technology Forecasts 2019-2029: IDTechEx," 2019.

[15] U. Rajendra Acharya, J. S. Suri, J. A. E. Spaan, and S. M. Krishnan, *Advances in Cardiac Signal Processing*. Berlin, Heidelberg: Springer Berlin Heidelberg, 2007.

[16] H. Naseri and M. R. Homaeinezhad, "Electrocardiogram signal quality assessment using an artificially reconstructed target lead," *Comput. Methods Biomech. Biomed. Engin.*, vol. 18, no. 10, pp. 1126–1141, Jul. 2015.

[17] E. Sazonov and M. R. Neuman, *Wearable sensors: Fundamentals, implementation and applications*. Academic Press, 2014.

[18] P. J. Xu, H. Zhang, and X. M. Tao, "Textile-structured electrodes for electrocardiogram," *Text. Prog.*, vol. 40, no. 4, pp. 183–213, Dec. 2008.

[19] GE Healthcare, "SEER 12 Digital Holter ECG Recorder - Ambulatory ECG." [Online]. Available: https://www.gehealthcare.co.uk/products/diagnostic-cardiology/ambulatory-ecg/seer-12-digital-holter-ecg-recorder. [Accessed: 18-Sep-2019].

[20] iRhythm, "Uninterrupted Ambulatory Cardiac Monitoring." [Online]. Available:

https://www.irhythmtech.com/. [Accessed: 08-Jan-2019].
[21] ZOLL Medical Corporation, “What Is the LifeVest Wearable Defibrillator?” [Online]. Available: https://lifevest.zoll.com/medical-professionals. [Accessed: 18-Sep-2019].
[22] Nuubo, “Nuubo.” [Online]. Available: https://www.nuubo.com/tecnologia. [Accessed: 18-Sep-2019].
[23] P. Perego, C. Standoli, and G. Andreoni, “Wearable monitoring of elderly in an ecologic setting: the SMARTA project,” in *Proceedings of 2nd International Electronic Conference on Sensors and Applications*, 2015, p. S3001.
[24] K. C. Tseng, Bor-Shyh Lin, Lun-De Liao, Yu-Te Wang, and Yu-Lin Wang, “Development of a Wearable Mobile Electrocardiogram Monitoring System by Using Novel Dry Foam Electrodes,” *IEEE Syst. J.*, vol. 8, no. 3, pp. 900–906, Sep. 2014.
[25] E. Nemati, M. Deen, and T. Mondal, “A wireless wearable ECG sensor for long-term applications,” *IEEE Commun. Mag.*, vol. 50, no. 1, pp. 36–43, Jan. 2012.
[26] J. Lee *et al.*, “Flexible Capacitive Electrodes for Minimizing Motion Artifacts in Ambulatory Electrocardiograms,” *Sensors*, vol. 14, no. 8, pp. 14732–14743, Aug. 2014.
[27] P. Fontana *et al.*, “Applicability of a Textile ECG-Belt for Unattended Sleep Apnoea Monitoring in a Home Setting,” *Sensors*, vol. 19, no. 15, p. 3367, Jul. 2019.
[28] P. Fontana *et al.*, “Clinical Applicability of a Textile 1-Lead ECG Device for Overnight Monitoring,” *Sensors*, vol. 19, no. 11, p. 2436, May 2019.
[29] M. Elliott, “Why is Respiratory Rate the Neglected Vital Sign? A Narrative Review,” *Int. Arch. Nurs. Heal. Care*, vol. 2, no. 3, Jun. 2016.
[30] K. Van Loon, B. Van Zaane, E. J. Bosch, C. J. Kalkman, and L. M. Peelen, “Non-invasive continuous respiratory monitoring on general hospital wards: A systematic review,” *PLoS ONE*, vol. 10, no. 12. Public Library of Science, p. e0144626, 14-Dec-2015.
[31] Y. Rabi, D. Kowal, and N. Ambalavanan, “Blood Gases: Technical Aspects and Interpretation,” in *Assisted Ventilation of the Neonate: An Evidence-Based Approach to Newborn Respiratory Care: Sixth Edition*, Elsevier, 2017, pp. 80-96.e3.
[32] B. Schoun, S. Transue, A. C. Halbower, and M. H. Choi, “Non-contact tidal volume measurement through thin medium thermal imaging,” *Smart Heal.*, vol. 9–10, pp. 37–49, Dec. 2018.
[33] A. F. Pacela, “Impedance pneumography-A survey of instrumentation techniques,” *Med. Biol. Eng.*, vol. 4, no. 1, pp. 1–15, Jan. 1966.
[34] V.-P. Seppa, J. Viik, and J. Hyttinen, “Assessment of Pulmonary Flow Using Impedance Pneumography,” *IEEE Trans. Biomed. Eng.*, vol. 57, no. 9, pp. 2277–2285, Sep. 2010.
[35] C. Massaroni, A. Nicolò, D. Lo Presti, M. Sacchetti, S. Silvestri, and E. Schena, “Contact-Based Methods for Measuring Respiratory Rate,” *Sensors*, vol. 19, no. 4, p. 908, Feb. 2019.
[36] M. Klum, T. Schenck, A. Pielmus, T. Tigges, and R. Orglmeister, “Short Distance Impedance Pneumography,” *Curr. Dir. Biomed. Eng.*, vol. 4, no. 1, pp. 109–113, Sep. 2018.
[37] P. H. Charlton *et al.*, “Extraction of respiratory signals from the electrocardiogram and photoplethysmogram: technical and physiological determinants,” *Physiol. Meas.*, vol. 38, no. 5, pp. 669–690, May 2017.
[38] J. Krishna, O. Sans-Capdevila, and D. Gozal, “Sleep studies: Which technologies?,” *Paediatr. Respir. Rev.*, vol. 7, no. SUPPL. 1, pp. S202–S205, Jan. 2006.
[39] Y. Retory, P. Niedzialkowski, C. de Picciotto, M. Bonay, and M. Petitjean, “New Respiratory Inductive Plethysmography (RIP) Method for Evaluating Ventilatory Adaptation during Mild Physical Activities,” *PLoS One*, vol. 11, no. 3, p. e0151983, Mar. 2016.
[40] G. Brüllmann, K. Fritsch, R. Thurnheer, and K. E. Bloch, “Respiratory Monitoring by Inductive Plethysmography in Unrestrained Subjects Using Position Sensor-Adjusted Calibration,”

Respiration, vol. 79, no. 2, pp. 112–120, 2010.

[41] P. Grossman, M. Spoerle, and F. H. Wilhelm, "Reliability of respiratory tidal volume estimation by means of ambulatory inductive plethysmography," in *Biomedical Sciences Instrumentation*, 2006, vol. 42, pp. 193–198.

[42] P. Grossman, F. H. Wilhelm, and M. Brutsche, "Accuracy of ventilatory measurement employing ambulatory inductive plethysmography during tasks of everyday life," *Biol. Psychol.*, vol. 84, no. 1, pp. 121–128, Apr. 2010.

[43] C. Massaroni, D. Lo Presti, D. Formica, S. Silvestri, and E. Schena, "Non-Contact Monitoring of Breathing Pattern and Respiratory Rate via RGB Signal Measurement," *Sensors*, vol. 19, no. 12, p. 2758, Jun. 2019.

[44] C. Massaroni, P. Saccomandi, and E. Schena, "Medical Smart Textiles Based on Fiber Optic Technology: An Overview," *J. Funct. Biomater.*, vol. 6, no. 2, pp. 204–221, Apr. 2015.

[45] M. D. Petrović *et al.*, "Non-invasive respiratory monitoring using long-period fiber grating sensors," *Biomed. Opt. Express*, vol. 5, no. 4, p. 1136, Apr. 2014.

[46] F. Narbonneau *et al.*, "Smart textile embedding optical fibre sensors for healthcare monitoring during MRI," in *CIMTEC 2008 - Proceedings of the 3rd International Conference on Smart Materials, Structures and Systems - Smart Textiles*, 2008, vol. 60, pp. 134–143.

[47] W. J. Yoo *et al.*, "Development of respiration sensors using plastic optical fiber for respiratory monitoring inside MRI system," *J. Opt. Soc. Korea*, vol. 14, no. 3, pp. 235–239, Sep. 2010.

[48] T. Allsop *et al.*, "Respiratory function monitoring using a real-time three-dimensional fiber-optic shaping sensing scheme based upon fiber Bragg gratings," *J. Biomed. Opt.*, vol. 17, no. 11, p. 117001, Nov. 2012.

[49] Y. Liu, S. H. Zhu, G. H. Wang, F. Ye, and P. Z. Li, "Validity and reliability of multiparameter physiological measurements recorded by the equivital lifemonitor during activities of various intensities," *J. Occup. Environ. Hyg.*, vol. 10, no. 2, pp. 78–85, Feb. 2013.

[50] Equivital, "Equivital." [Online]. Available: http://www.equivital.com/. [Accessed: 13-Jan-2019].

[51] J. D. Witt, J. R. K. O. Fisher, J. A. Guenette, K. A. Cheong, B. J. Wilson, and A. W. Sheel, "Measurement of exercise ventilation by a portable respiratory inductive plethysmograph," *Respir. Physiol. Neurobiol.*, vol. 154, no. 3, pp. 389–395, Dec. 2006.

[52] Zephyr™, "Components | Zephyr™ Performance Systems." [Online]. Available: https://www.zephyranywhere.com/system/components. [Accessed: 20-Sep-2019].

[53] J. H. Kim, R. Roberge, J. B. Powell, A. B. Shafer, and W. Jon Williams, "Measurement accuracy of heart rate and respiratory rate during graded exercise and sustained exercise in the heat using the zephyr BioHarness TM," *Int. J. Sports Med.*, vol. 34, no. 6, pp. 497–501, Nov. 2013.

[54] Carre Technologies Inc (Hexoskin), "Hexoskin Smart Shirts." [Online]. Available: https://www.hexoskin.com/. [Accessed: 20-Sep-2019].

[55] M. Holt, B. Yule, D. Jackson, M. Zhu, and N. Moraveji, "Ambulatory monitoring of respiratory effort using a clothing-adhered biosensor," in *2018 IEEE International Symposium on Medical Measurements and Applications (MeMeA)*, 2018, pp. 1–6.

[56] J. M. Purswani, N. Ohri, and C. Champ, "Tracking steps in oncology: the time is now," *Cancer Manag. Res.*, vol. 10, pp. 2439–2447, Aug. 2018.

[57] M. S. Beg, A. Gupta, T. Stewart, and C. D. Rethorst, "Promise of Wearable Physical Activity Monitors in Oncology Practice," *J. Oncol. Pract.*, vol. 13, no. 2, pp. 82–89, Feb. 2017.

[58] W. K. Lim *et al.*, "Beyond fitness tracking: The use of consumer-grade wearable data from normal volunteers in cardiovascular and lipidomics research," *PLOS Biol.*, vol. 16, no. 2, p. e2004285, Feb. 2018.

[59] D. R. Bassett, L. P. Toth, S. R. LaMunion, and S. E. Crouter, "Step Counting: A Review of

Measurement Considerations and Health-Related Applications," *Sport. Med.*, vol. 47, no. 7, pp. 1303–1315, Jul. 2017.

[60] H. Van Remoortel *et al.*, "Validity of activity monitors in health and chronic disease: a systematic review," *Int. J. Behav. Nutr. Phys. Act.*, vol. 9, no. 1, p. 84, 2012.

[61] M. J. Mathie, A. C. F. Coster, N. H. Lovell, and B. G. Celler, "Accelerometry: providing an integrated, practical method for long-term, ambulatory monitoring of human movement," *Physiol. Meas.*, vol. 25, no. 2, pp. R1–R20, Apr. 2004.

[62] D. Naranjo-Hernandez, L. M. Roa, J. Reina-Tosina, and M. A. Estudillo-Valderrama, "SoM: A Smart Sensor for Human Activity Monitoring and Assisted Healthy Ageing," *IEEE Trans. Biomed. Eng.*, vol. 59, no. 11, pp. 3177–3184, Nov. 2012.

[63] Y. Kishimoto, Y. Kutsuna, and K. Oguri, "Detecting Motion Artifact ECG Noise During Sleeping by Means of a Tri-axis Accelerometer," in *2007 29th Annual International Conference of the IEEE Engineering in Medicine and Biology Society*, 2007, pp. 2669–2672.

[64] M. Šimaitytė, A. Petrėnas, J. Kravčenko, E. Kaldoudi, and V. Marozas, "Objective evaluation of physical activity pattern using smart devices," *Sci. Rep.*, vol. 9, no. 1, p. 2006, Dec. 2019.

[65] T. Althoff, R. Sosič, J. L. Hicks, A. C. King, S. L. Delp, and J. Leskovec, "Large-scale physical activity data reveal worldwide activity inequality," *Nature*, vol. 547, no. 7663, pp. 336–339, Jul. 2017.

[66] J. T. Cavanaugh, K. L. Coleman, J. M. Gaines, L. Laing, and M. C. Morey, "Using Step Activity Monitoring to Characterize Ambulatory Activity in Community-Dwelling Older Adults," *J. Am. Geriatr. Soc.*, vol. 55, no. 1, pp. 120–124, Jan. 2007.

[67] S. Ortlieb *et al.*, "Exploring patterns of accelerometry-assessed physical activity in elderly people," *Int. J. Behav. Nutr. Phys. Act.*, vol. 11, no. 1, p. 28, 2014.

[68] J. Fridolfsson *et al.*, "Effects of Frequency Filtering on Intensity and Noise in Accelerometer-Based Physical Activity Measurements," *Sensors*, vol. 19, no. 9, p. 2186, May 2019.

[69] V. H. Rodriguez, C. Medrano, I. Plaza, C. Corella, A. Abarca, and J. A. Julian, "Comparison of Several Algorithms to Estimate Activity Counts with Smartphones as an Indication of Physical Activity Level," *IRBM*, vol. 40, no. 2, pp. 95–102, Mar. 2019.

[70] A. Doherty *et al.*, "Large Scale Population Assessment of Physical Activity Using Wrist Worn Accelerometers: The UK Biobank Study," *PLoS One*, vol. 12, no. 2, p. e0169649, Feb. 2017.

[71] A. Hecht, S. Ma, J. Porszasz, R. Casaburi, and for the COPD Clinical Research Netw, "Methodology for Using Long-Term Accelerometry Monitoring to Describe Daily Activity Patterns in COPD," *COPD J. Chronic Obstr. Pulm. Dis.*, vol. 6, no. 2, pp. 121–129, Jan. 2009.

[72] S. F. M. Chastin and M. H. Granat, "Methods for objective measure, quantification and analysis of sedentary behaviour and inactivity," *Gait Posture*, vol. 31, no. 1, pp. 82–86, Jan. 2010.

[73] A. V. Rowlands, C. L. Edwardson, M. J. Davies, K. Khunti, D. M. Harrington, and T. Yates, "Beyond Cut Points: Accelerometer Metrics that Capture the Physical Activity Profile," *Med. Sci. Sports Exerc.*, vol. 50, no. 6, pp. 1323–1332, Jun. 2018.

[74] Fitbit Inc, "Fitbit Official Site for Activity Trackers and More." [Online]. Available: https://www.fitbit.com/eu/home. [Accessed: 22-Sep-2019].

[75] Cloud DX, "Cloud DX | VITALITI." [Online]. Available: https://www.clouddx.com/#/vitaliti. [Accessed: 09-Jan-2019].

[76] U.S. Food and Drug Administration, "510(k) Premarket Notification." [Online]. Available: https://www.accessdata.fda.gov/scripts/cdrh/cfdocs/cfPMN/pmn.cfm. [Accessed: 22-Sep-2019].

[77] J. Selvaraj, M. Murugappan, K. Wan, and S. Yaacob, "Classification of emotional states from electrocardiogram signals: A non-linear approach based on hurst," *Biomed. Eng. Online*, vol. 12, no. 1, p. 44, May 2013.

[78] S. Brás, J. H. T. Ferreira, S. C. Soares, and A. J. Pinho, “Biometric and Emotion Identification: An ECG Compression Based Method,” *Front. Psychol.*, vol. 9, no. APR, p. 467, Apr. 2018.

[79] The MathWorks Inc., “Real-Time ECG QRS Detection,” 2018. [Online]. Available: https://www.mathworks.com/help/dsp/examples/real-time-ecg-qrs-detection.html. [Accessed: 12-Sep-2019].

[80] N. Kannathal, U. R. Acharya, K. P. Joseph, L. C. Min, and J. S. Suri, “Analysis of Electrocardiograms,” in *Advances in Cardiac Signal Processing*, Berlin, Heidelberg: Springer Berlin Heidelberg, 2007, pp. 55–82.

[81] S. Kaplan Berkaya, A. K. Uysal, E. Sora Gunal, S. Ergin, S. Gunal, and M. B. Gulmezoglu, “A survey on ECG analysis,” *Biomed. Signal Process. Control*, vol. 43, no. 1, pp. 216–235, May 2018.

[82] T. Penzel, J. McNames, P. de Chazal, B. Raymond, A. Murray, and G. Moody, “Systematic comparison of different algorithms for apnoea detection based on electrocardiogram recordings,” *Med. Biol. Eng. Comput.*, vol. 40, no. 4, pp. 402–407, Jul. 2002.

[83] M. J. Lado, A. J. Méndez, L. Rodríguez-Liñares, A. Otero, and X. A. Vila, “Nocturnal evolution of heart rate variability indices in sleep apnea.,” *Comput. Biol. Med.*, vol. 42, no. 12, pp. 1179–85, Dec. 2012.

[84] Y. Takemura, J. Sato, and M. Nakajima, “A Respiratory Movement Monitoring System Using Fiber-Grating Vision Sensor for Diagnosing Sleep Apnea Syndrome,” *Opt. Rev.*, vol. 12, no. 1, pp. 46–53, Jan. 2005.

[85] R. B. Berry *et al.*, “Rules for Scoring Respiratory Events in Sleep: Update of the 2007 AASM Manual for the Scoring of Sleep and Associated Events,” *J. Clin. Sleep Med.*, vol. 8, no. 5, pp. 597–619, Oct. 2012.

[86] American Academy of Sleep Medicine Task Force, “Sleep–Related Breathing Disorders in Adults: Recommendations for Syndrome Definition and Measurement Techniques in Clinical Research,” *Sleep*, vol. 22, no. 5, pp. 667–689, Aug. 1999.

[87] M. Hardinge, “Obstructive sleep apnoea,” *Medicine (Baltimore).*, vol. 36, no. 5, pp. 237–241, May 2008.

[88] D. Álvarez, R. Hornero, D. Abásolo, F. del Campo, and C. Zamarrón, “Nonlinear characteristics of blood oxygen saturation from nocturnal oximetry for obstructive sleep apnoea detection,” *Physiol. Meas.*, vol. 27, no. 4, pp. 399–412, Apr. 2006.

[89] H. Jin *et al.*, “Acoustic Analysis of Snoring in the Diagnosis of Obstructive Sleep Apnea Syndrome: A Call for More Rigorous Studies,” *J. Clin. Sleep Med.*, vol. 11, no. 7, pp. 765–71, Jul. 2015.

[90] M. J. Lado, A. J. Méndez, L. Rodríguez-Liñares, A. Otero, and X. A. Vila, “Nocturnal evolution of heart rate variability indices in sleep apnea,” *Comput. Biol. Med.*, vol. 42, no. 12, pp. 1179–1185, Dec. 2012.

[91] C. Orphanidou, “Quality Assessment for the Electrocardiogram (ECG),” in *Signal Quality Assessment in Physiological Monitoring*, 2018, pp. 15–40.

[92] L. Sörnmo and P. Laguna, “The Electrocardiogram—A Brief Background,” in *Bioelectrical Signal Processing in Cardiac and Neurological Applications*, Elsevier, 2005, pp. 411–452.

[93] G. M. Friesen, T. C. Jannett, M. A. Jadallah, S. L. Yates, S. R. Quint, and H. T. Nagle, “A Comparison of the Noise Sensitivity of Nine QRS Detection Algorithms,” *IEEE Trans. Biomed. Eng.*, vol. 37, no. 1, pp. 85–98, 1990.

[94] C. Levkov, G. Mihov, R. Ivanov, I. Daskalov, I. Christov, and I. Dotsinsky, “Removal of power-line interference from the ECG: a review of the subtraction procedure.,” *Biomed. Eng. Online*, vol. 4, p. 50, Aug. 2005.

[95] L. Johannesen, “Assessment of ECG quality on an android platform,” in *Computing in*

Cardiology, 2011, vol. 38, pp. 433–436.
[96] D. Hayn, B. Jammerbund, and G. Schreier, "ECG quality assessment for patient empowerment in mHealth applications," in *Computing in Cardiology*, 2011, vol. 38, pp. 353–356.
[97] U. Satija, B. Ramkumar, and S. M. Manikandan, "Real-Time Signal Quality-Aware ECG Telemetry System for IoT-Based Health Care Monitoring," *IEEE Internet Things J.*, vol. 4, no. 3, pp. 815–823, Jun. 2017.
[98] P. Castiglioni, P. Meriggi, A. Faini, and M. Di Rienzo, "Cepstral based approach for online quantification of ECG quality in freely moving subjects," in *Computing in Cardiology*, 2011, vol. 38, pp. 625–628.
[99] S. Zaunseder, R. Huhle, and H. Malberg, "CinC challenge - Assessing the usability of ECG by ensemble decision trees," in *Computing in Cardiology*, 2011, vol. 38, pp. 277–280.
[100] C. Orphanidou, T. Bonnici, P. Charlton, D. Clifton, D. Vallance, and L. Tarassenko, "Signal Quality Indices for the Electrocardiogram and Photoplethysmogram: Derivation and Applications to Wireless Monitoring," *IEEE J. Biomed. Heal. Informatics*, vol. 55, no. 11, pp. 1–1, 2014.
[101] D. Nabil and F. Bereksi Reguig, "Ectopic beats detection and correction methods: A review," *Biomed. Signal Process. Control*, vol. 18, no. 2, pp. 228–244, Apr. 2015.
[102] J. Behar, J. Oster, Qiao Li, and G. D. Clifford, "ECG Signal Quality During Arrhythmia and Its Application to False Alarm Reduction," *IEEE Trans. Biomed. Eng.*, vol. 60, no. 6, pp. 1660–1666, Jun. 2013.
[103] S. Gholinezhadasnefestani, A. Temko, N. Stevenson, G. Boylan, G. Lightbody, and W. Marnane, "Assessment of quality of ECG for accurate estimation of Heart Rate Variability in newborns," in *Proceedings of the Annual International Conference of the IEEE Engineering in Medicine and Biology Society, EMBS*, 2015, vol. 2015-Novem, pp. 5863–5866.
[104] D. Hayn, B. Jammerbund, and G. Schreier, "QRS detection based ECG quality assessment," *Physiol. Meas.*, vol. 33, no. 9, pp. 1449–1461, Sep. 2012.
[105] C. Orphanidou and I. Drobnjak, "Quality Assessment of Ambulatory ECG Using Wavelet Entropy of the HRV Signal," *IEEE J. Biomed. Heal. Informatics*, vol. 21, no. 5, pp. 1216–1223, Sep. 2017.
[106] A. S. Al-Fahoum, "Quality Assessment of ECG Compression Techniques Using a Wavelet-Based Diagnostic Measure," *IEEE Trans. Inf. Technol. Biomed.*, vol. 10, no. 1, pp. 182–191, Jan. 2006.
[107] C. Liu, P. Li, L. Zhao, F. Liu, and R. Wang, "Real-time Signal Quality Assessment for ECGs Collected Using Mobile Phones," in *Computing in Cardiology*, 2011, pp. 357–360.
[108] G. Chen, Z. Hong, Y. Guo, and C. Pang, "A cascaded classifier for multi-lead ECG based on feature fusion," *Comput. Methods Programs Biomed.*, vol. 178, pp. 135–143, Sep. 2019.
[109] G. D. Clifford, J. Behar, Q. Li, and I. Rezek, "Signal quality indices and data fusion for determining clinical acceptability of electrocardiograms," *Physiol. Meas.*, vol. 33, no. 9, pp. 1419–1433, Sep. 2012.
[110] H. Xia *et al.*, "Computer algorithms for evaluating the quality of ECGs in real time," in *Computing in Cardiology*, 2011, vol. 38, pp. 369–372.
[111] C. Daluwatte, L. Johannesen, L. Galeotti, J. Vicente, D. G. Strauss, and C. G. Scully, "Assessing ECG signal quality indices to discriminate ECGs with artefacts from pathologically different arrhythmic ECGs," *Physiol. Meas.*, vol. 37, no. 8, pp. 1370–1382, Aug. 2016.
[112] N. Patel, C. Donahue, A. Shenoy, A. Patel, and N. El-Sherif, "Obstructive sleep apnea and arrhythmia: A systemic review," *Int. J. Cardiol.*, vol. 228, pp. 967–970, Feb. 2017.
[113] M. Brennan, M. Palaniswami, and P. Kamen, "Do existing measures of Poincare plot geometry reflect nonlinear features of heart rate variability?," *IEEE Trans. Biomed. Eng.*, vol. 48, no. 11,

pp. 1342–1347, Nov. 2001.
[114] M. A. Woo, W. G. Stevenson, D. K. Moser, R. B. Trelease, and R. M. Harper, “Patterns of beat-to-beat heart rate variability in advanced heart failure,” *Am. Heart J.*, vol. 123, no. 3, pp. 704–710, Mar. 1992.
[115] L. Mourot *et al.*, “Decrease in heart rate variability with overtraining: assessment by the Poincare plot analysis,” *Clin. Physiol. Funct. Imaging*, vol. 24, no. 1, pp. 10–18, Jan. 2004.
[116] J. Piskorski and P. Guzik, “Filtering Poincaré plots,” *Comput. Methods Sci. Technol.*, vol. 11, no. 1, pp. 39–48, 2005.
[117] A. K. Golińska, “Poincaré Plots in Analysis of Selected Biomedical Signals,” *Stud. Logic, Gramm. Rhetor.*, vol. 35, no. 1, pp. 117–127, Dec. 2013.
[118] J. Piskorski and P. Guzik, “Geometry of the Poincaré plot of RR intervals and its asymmetry in healthy adults.,” *Physiol. Meas.*, vol. 28, no. 3, pp. 287–300, Mar. 2007.
[119] N. J. C. Stapelberg, D. L. Neumann, D. H. K. Shum, H. McConnell, and I. Hamilton-Craig, “The sensitivity of 38 heart rate variability measures to the addition of artifact in human and artificial 24-hr cardiac recordings,” *Ann. Noninvasive Electrocardiol.*, vol. 23, no. 1, p. e12483, Jan. 2018.
[120] M. A. Woo, W. G. Stevenson, D. K. Moser, and H. R. Middlekauff, “Complex heart rate variability and serum norepinephrine levels in patients with advanced heart failure,” *J. Am. Coll. Cardiol.*, vol. 23, no. 3, pp. 565–569, Mar. 1994.
[121] World Health Organization, *Global Recommendations on Physical Activity for Health*. WHO Press, 2010.
[122] M. Niemelä *et al.*, “Intensity and temporal patterns of physical activity and cardiovascular disease risk in midlife,” *Prev. Med. (Baltim).*, vol. 124, pp. 33–41, Jul. 2019.
[123] S. Lachman *et al.*, “Impact of physical activity on the risk of cardiovascular disease in middle-aged and older adults: EPIC Norfolk prospective population study,” *Eur. J. Prev. Cardiol.*, vol. 25, no. 2, pp. 200–208, Jan. 2018.
[124] H. W. Kohl, “Physical activity and cardiovascular disease: evidence for a dose response.,” *Med. Sci. Sports Exerc.*, vol. 33, no. 6 Suppl, pp. S472-83; discussion S493-4, Jun. 2001.
[125] H. Arem *et al.*, “Leisure Time Physical Activity and Mortality,” *JAMA Intern. Med.*, vol. 175, no. 6, p. 959, Jun. 2015.
[126] S. E. Baumeister *et al.*, “Association between physical activity and risk of hepatobiliary cancers: A multinational cohort study,” *J. Hepatol.*, vol. 70, no. 5, pp. 885–892, May 2019.
[127] N. Fluetsch, C. Levy, and L. Tallon, “The relationship of physical activity to mental health: A 2015 behavioral risk factor surveillance system data analysis,” *J. Affect. Disord.*, vol. 253, pp. 96–101, Jun. 2019.
[128] A. J. Halliday, M. L. Kern, and D. A. Turnbull, “Can physical activity help explain the gender gap in adolescent mental health? A cross-sectional exploration,” *Ment. Health Phys. Act.*, vol. 16, pp. 8–18, Mar. 2019.
[129] B. Gavilán-Carrera *et al.*, “Association of objectively measured physical activity and sedentary time with health-related quality of life in women with fibromyalgia: The al-Ándalus project,” *J. Sport Heal. Sci.*, vol. 8, no. 3, pp. 258–266, May 2019.
[130] K. Sharif, A. Watad, N. L. Bragazzi, M. Lichtbroun, H. Amital, and Y. Shoenfeld, “Physical activity and autoimmune diseases: Get moving and manage the disease,” *Autoimmun. Rev.*, vol. 17, no. 1, pp. 53–72, Jan. 2018.
[131] S. Pradhan and V. E. Kelly, “Quantifying physical activity in early Parkinson disease using a commercial activity monitor,” *Parkinsonism Relat. Disord.*, vol. 66, pp. 171–175, Sep. 2019.
[132] M. Naghavi *et al.*, “Global, regional, and national age-sex specific mortality for 264 causes of death, 1980–2016: a systematic analysis for the Global Burden of Disease Study 2016,” *Lancet*, vol. 390, no. 10100, pp. 1151–1210, Sep. 2017.

[133] D. Ndahimana and E.-K. Kim, “Measurement Methods for Physical Activity and Energy Expenditure: a Review,” *Clin. Nutr. Res.*, vol. 6, no. 2, p. 68, 2017.
[134] Y. Y. Lam and E. Ravussin, “Analysis of energy metabolism in humans: A review of methodologies,” *Mol. Metab.*, vol. 5, no. 11, pp. 1057–1071, Nov. 2016.
[135] K. L. Canning, R. E. Brown, V. K. Jamnik, A. Salmon, C. I. Ardern, and J. L. Kuk, “Individuals Underestimate Moderate and Vigorous Intensity Physical Activity,” *PLoS One*, vol. 9, no. 5, p. e97927, May 2014.
[136] K. Vassbakk-Brovold *et al.*, “Cancer patients participating in a lifestyle intervention during chemotherapy greatly over-report their physical activity level: a validation study,” *BMC Sports Sci. Med. Rehabil.*, vol. 8, no. 1, p. 10, Dec. 2016.
[137] Z. Silsbury, R. Goldsmith, and A. Rushton, “Systematic review of the measurement properties of self-report physical activity questionnaires in healthy adult populations: Figure 1,” *BMJ Open*, vol. 5, no. 9, p. e008430, Sep. 2015.
[138] J. A. Levine, “Measurement of energy expenditure,” *Public Health Nutr.*, vol. 8, no. 7a, pp. 1123–1132, Oct. 2005.
[139] J. Achten and A. E. Jeukendrup, “Heart Rate Monitoring,” *Sport. Med.*, vol. 33, no. 7, pp. 517–538, 2003.
[140] M. B. Livingstone, P. J. Robson, and M. Totton, “Energy expenditure by heart rate in children: an evaluation of calibration techniques.,” *Med. Sci. Sports Exerc.*, vol. 32, no. 8, pp. 1513–9, Aug. 2000.
[141] Z. Yu *et al.*, “Comparison of heart rate monitoring with indirect calorimetry for energy expenditure evaluation,” *J. Sport Heal. Sci.*, vol. 1, no. 3, pp. 178–183, Dec. 2012.
[142] A. P. Welles, M. J. Buller, D. P. Looney, W. V. Rumpler, A. V. Gribok, and R. W. Hoyt, “Estimation of metabolic energy expenditure from core temperature using a human thermoregulatory model,” *J. Therm. Biol.*, vol. 72, pp. 44–52, Feb. 2018.
[143] R. Gilgen-Ammann, M. Koller, C. Huber, R. Ahola, T. Korhonen, and T. Wyss, “Energy expenditure estimation from respiration variables,” *Sci. Rep.*, vol. 7, no. 1, p. 15995, Dec. 2017.
[144] J. V. G. A. Durnin and R. G. Edwards, “PULMONARY VENTILATION AS AN INDEX OF ENERGY EXPENDITURE,” *Q. J. Exp. Physiol. Cogn. Med. Sci.*, vol. 40, no. 4, pp. 370–377, Oct. 1955.
[145] W. R. Leonard, “Measuring human energy expenditure: What have we learned from the flex-heart rate method?,” *Am. J. Hum. Biol.*, vol. 15, no. 4, pp. 479–489, Jun. 2003.
[146] J. A. Schrack, V. Zipunnikov, J. Goldsmith, K. Bandeen-Roche, C. M. Crainiceanu, and L. Ferrucci, “Estimating Energy Expenditure from Heart Rate in Older Adults: A Case for Calibration,” *PLoS One*, vol. 9, no. 4, p. e93520, Apr. 2014.
[147] L. S. Pescatello and American College of Sports Medicine., *ACSM’s guidelines for exercise testing and prescription*, 9th ed. Wolters Kluwer/Lippincott Williams & Wilkins Health, 2014.
[148] V. K. Jamnik *et al.*, “Enhancing the effectiveness of clearance for physical activity participation: background and overall process,” *Appl. Physiol. Nutr. Metab.*, vol. 36, no. S1, pp. S3–S13, Jul. 2011.
[149] M. Abel, J. Hannon, D. Mullineaux, and A. Beighle, “Determination of step rate thresholds corresponding to physical activity intensity classifications in adults.,” *J. Phys. Act. Health*, vol. 8, no. 1, pp. 45–51, Jan. 2011.
[150] C. Tudor-Locke *et al.*, “Cadence (steps/min) and intensity during ambulation in 6-20 year olds: The CADENCE-kids study,” *Int. J. Behav. Nutr. Phys. Act.*, vol. 15, no. 1, p. 20, Dec. 2018.
[151] C. Tudor-Locke *et al.*, “Walking cadence (steps/min) and intensity in 21–40 year olds: CADENCE-adults,” *Int. J. Behav. Nutr. Phys. Act.*, vol. 16, no. 1, p. 8, Dec. 2019.
[152] A. Fernandez and D. Dang, “Analog,” in *Getting Started with the MSP430 Launchpad*, Elsevier,

2013, pp. 81–125.
[153] K. R. Westerterp, “Assessment of physical activity: a critical appraisal,” *Eur. J. Appl. Physiol.*, vol. 105, no. 6, pp. 823–828, Apr. 2009.
[154] S. E. Crouter, J. R. Churilla, and D. R. Bassett, “Estimating energy expenditure using accelerometers.,” *Eur. J. Appl. Physiol.*, vol. 98, no. 6, pp. 601–12, Dec. 2006.
[155] F.-P. Alberto, M. Nathanael, B. Mathew, and B. E. Ainsworth, “Wearable monitors criterion validity for energy expenditure in sedentary and light activities,” *J. Sport Heal. Sci.*, vol. 6, no. 1, pp. 103–110, Mar. 2017.
[156] R. S. Sacko *et al.*, “Comparison of Indirect Calorimetry- and Accelerometry-Based Energy Expenditure during Object Project Skill Performance,” *Meas. Phys. Educ. Exerc. Sci.*, vol. 23, no. 2, pp. 148–158, Apr. 2019.
[157] D. Hendelman, K. Miller, C. Baggett, E. Debold, and P. Freedson, “Validity of accelerometry for the assessment of moderate intensity physical activity in the field,” *Med. Sci. Sports Exerc.*, vol. 32, no. 9 SUPPL., pp. S442–S449, Sep. 2000.
[158] World Health Organization, “WHO | What is Moderate-intensity and Vigorous-intensity Physical Activity?,” *WHO*, 2014. [Online]. Available: https://www.who.int/dietphysicalactivity/physical_activity_intensity/en/. [Accessed: 04-Apr-2019].
[159] A. Nicolò, C. Massaroni, and L. Passfield, “Respiratory Frequency during Exercise: The Neglected Physiological Measure,” *Front. Physiol.*, vol. 8, no. DEC, p. 922, Dec. 2017.
[160] A. Nicolò, I. Bazzucchi, J. Haxhi, F. Felici, and M. Sacchetti, “Comparing Continuous and Intermittent Exercise: An ‘Isoeffort’ and ‘Isotime’ Approach,” *PLoS One*, vol. 9, no. 4, p. e94990, Apr. 2014.
[161] P. S. Freedson, E. Melanson, and J. Sirard, “Calibration of the Computer Science and Applications, Inc. accelerometer.,” *Med. Sci. Sports Exerc.*, vol. 30, no. 5, pp. 777–81, May 1998.
[162] J. A. Bell, M. Hamer, V. T. Van Hees, A. Singh-Manoux, M. Kivimäki, and S. Sabia, “Healthy obesity and objective physical activity,” *Am. J. Clin. Nutr.*, vol. 102, no. 2, pp. 268–275, Aug. 2015.
[163] Y. Kim, T. White, K. Wijndaele, S. J. Sharp, N. J. Wareham, and S. Brage, “Adiposity and grip strength as long-term predictors of objectively measured physical activity in 93 015 adults: the UK Biobank study,” *Int. J. Obes.*, vol. 41, no. 9, pp. 1361–1368, Sep. 2017.
[164] J. Fatisson, V. Oswald, and F. Lalonde, “Influence diagram of physiological and environmental factors affecting heart rate variability: An extended literature overview,” *Heart International*, vol. 11, no. 1. SAGE PublicationsSage UK: London, England, pp. e32–e40, 25-Jan-2016.
[165] M. Li, K.-C. Kwak, and Y. Kim, “Estimation of Energy Expenditure Using a Patch-Type Sensor Module with an Incremental Radial Basis Function Neural Network,” *Sensors*, vol. 16, no. 10, p. 1566, Sep. 2016.
[166] S. J. Strath, D. R. Bassett, A. M. Swartz, and D. L. Thompson, “Simultaneous heart rate-motion sensor technique to estimate energy expenditure.,” *Med. Sci. Sports Exerc.*, vol. 33, no. 12, pp. 2118–23, Dec. 2001.
[167] J. J. Kraal *et al.*, “Energy expenditure estimation in beta-blocker-medicated cardiac patients by combining heart rate and body movement data,” *Eur. J. Prev. Cardiol.*, vol. 23, no. 16, pp. 1734–1742, Nov. 2016.
[168] K. Lu, L. Yang, F. Seoane, F. Abtahi, M. Forsman, and K. Lindecrantz, “Fusion of Heart Rate, Respiration and Motion Measurements from a Wearable Sensor System to Enhance Energy Expenditure Estimation,” *Sensors*, vol. 18, no. 9, p. 3092, Sep. 2018.
[169] F. Taffoni, D. Rivera, A. La Camera, A. Nicolò, J. R. Velasco, and C. Massaroni, “A Wearable System for Real-Time Continuous Monitoring of Physical Activity,” *J. Healthc. Eng.*, vol. 2018,

pp. 1–16, Mar. 2018.
[170] H. Gjoreski, B. Kaluža, M. Gams, R. Milić, and M. Luštrek, “Ensembles of multiple sensors for human energy expenditure estimation,” in *UbiComp 2013 - Proceedings of the 2013 ACM International Joint Conference on Pervasive and Ubiquitous Computing*, 2013, pp. 359–362.
[171] D. Curone, G. M. Bertolotti, A. Cristiani, E. L. Secco, and G. Magenes, “A Real-Time and Self-Calibrating Algorithm Based on Triaxial Accelerometer Signals for the Detection of Human Posture and Activity,” *IEEE Trans. Inf. Technol. Biomed.*, vol. 14, no. 4, pp. 1098–1105, Jul. 2010.
[172] H. Ichijo and M. Akita, “Gender difference and laterality of sleep position,” *Auris Nasus Larynx*, vol. 45, no. 3, pp. 592–597, Jun. 2018.
[173] G. D. Pinna *et al.*, “Differential impact of body position on the severity of disordered breathing in heart failure patients with obstructive vs. central sleep apnoea,” *Eur. J. Heart Fail.*, vol. 17, no. 12, pp. 1302–1309, Dec. 2015.
[174] L. Coutier, A. Guyon, P. Reix, and P. Franco, “Impact of prone positioning in infants with Pierre Robin sequence: a polysomnography study,” *Sleep Med.*, vol. 54, pp. 257–261, Feb. 2019.
[175] H. Gjoreski and M. Gams, “Activity/Posture Recognition using Wearable Sensors Placed on Different Body Locations,” in *Signal and Image Processing and Applications / 716: Artificial Intelligence and Soft Computing*, 2011.
[176] M. Mao, Y. Chuo, and B. Kaminska, “Multi-functional Wearable Device for Heart Health and Position Assessment,” *Nsti Nanotech 2008, Vol 2, Tech. Proc.*, vol. 2, pp. 615–618, 2008.
[177] M. Nazarahari and H. Rouhani, “Detection of daily postures and walking modalities using a single chest-mounted tri-axial accelerometer,” *Med. Eng. Phys.*, vol. 57, pp. 75–81, Jul. 2018.
[178] A. M. Khan, Y.-K. Lee, S. Y. Lee, and T.-S. Kim, “A triaxial accelerometer-based physical-activity recognition via augmented-signal features and a hierarchical recognizer.,” *IEEE Trans. Inf. Technol. Biomed.*, vol. 14, no. 5, pp. 1166–72, Sep. 2010.
[179] V. Lugade, E. Fortune, M. Morrow, and K. Kaufman, “Validity of using tri-axial accelerometers to measure human movement-Part I: Posture and movement detection,” *Med. Eng. Phys.*, vol. 36, no. 2, pp. 169–176, Feb. 2014.
[180] G. M. Lyons, K. M. Culhane, D. Hilton, P. A. Grace, and D. Lyons, “A description of an accelerometer-based mobility monitoring technique,” *Med. Eng. Phys.*, vol. 27, no. 6, pp. 497–504, Jul. 2005.

Appendix A. ECG monitoring in a home setting

Table A1. Signal quality indices of the 28 nights.

Subject	Night	Artefact percentage	SNR_{hf}	SNR_{lf}	BLW	SD1	SD2	SD1/SD2
			dB	dB	mV	ms	ms	ms
112	1	1.1%	27	7	0.001	38.8	187.1	0.21
121	2	11.3%	4	14	0.002	34.8	68.5	0.51
121	3	7.0%	23	12	0.003	17.8	86.4	0.21
121	4	4.0%	24	10	0.004	24.0	101.8	0.24
129	5	2.6%	21	6	0.005	28.0	169.6	0.17
129	6	0.9%	20	13	0.006	17.2	127.1	0.14
129	7	1.3%	20	10	0.007	20.5	142.0	0.14
133	8	0.2%	24	12	0.008	20.5	97.9	0.21
133	9	0.3%	23	10	0.009	19.0	100.8	0.19
133	10	0.3%	23	9	0.010	14.1	98.9	0.14
155	11	1.4%	19	15	0.011	34.4	157.3	0.22
160	12	47.8%	26	8	0.012	82.5	227.5	0.36
160	13	27.4%	23	9	0.013	50.8	156.2	0.33
161	14	0.2%	21	13	0.014	15.5	97.9	0.16
161	15	0.3%	17	11	0.015	13.9	95.2	0.15
161	16	0.2%	21	12	0.016	17.2	85.5	0.20
166	17	0.6%	17	9	0.017	11.4	74.5	0.15
166	18	6.2%	16	11	0.018	26.9	80.6	0.33
166	19	5.0%	15	11	0.019	16.4	105.5	0.16
168	20	0.6%	24	10	0.020	26.9	176.4	0.15
168	21	0.6%	24	13	0.021	26.3	181.7	0.15
168	22	0.9%	24	11	0.022	31.4	151.7	0.21
186	23	12.2%	26	12	0.023	80.0	179.3	0.45
206	24	7.3%	18	9	0.024	22.1	129.2	0.17
206	25	6.2%	20	11	0.025	33.4	119.9	0.28
206	26	10.3%	20	12	0.026	32.8	127.3	0.26
228	27	15.1%	26	9	0.027	53.7	192.8	0.28
228	28	15.8%	25	9	0.028	53.6	132.1	0.41

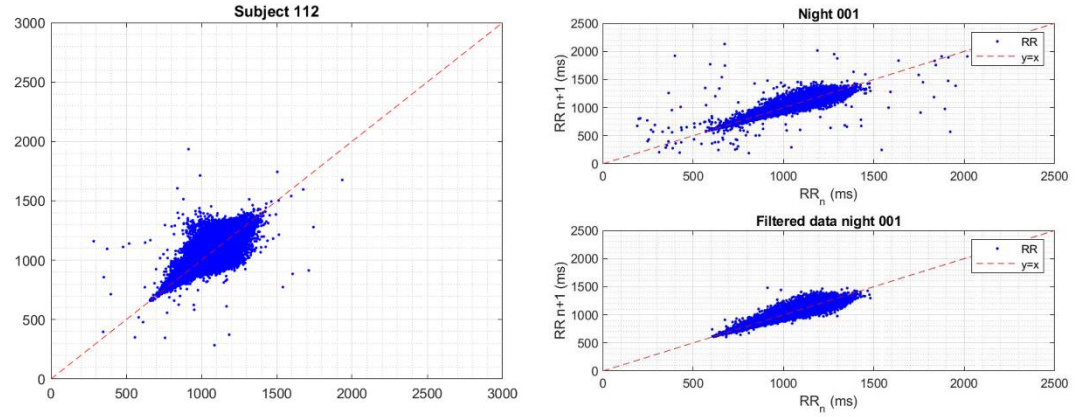

Figure A1. Poincaré plot of subject 112. Data acquired by the gel electrodes during the clinical study (left), and data acquired in the home setting (right).

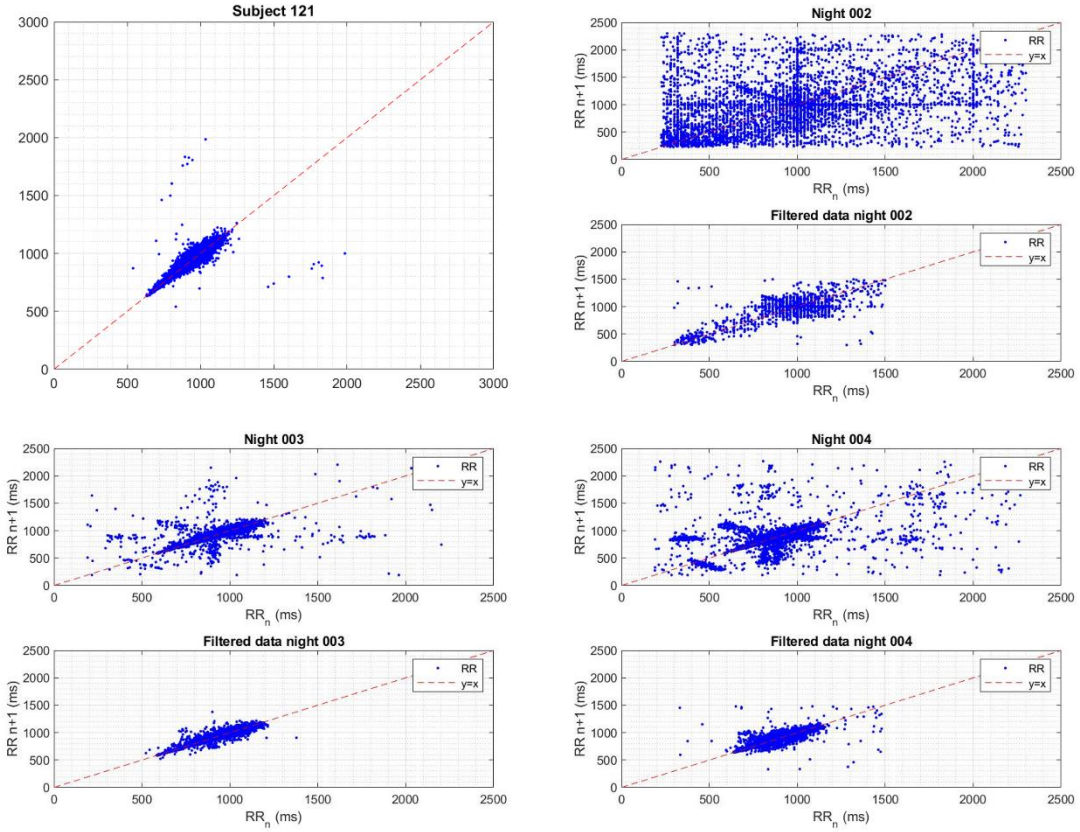

Figure A2. Poincaré plot of subject 121. Data acquired by the gel electrodes during the clinical study (top, left), and data acquired in the home setting (remainder).

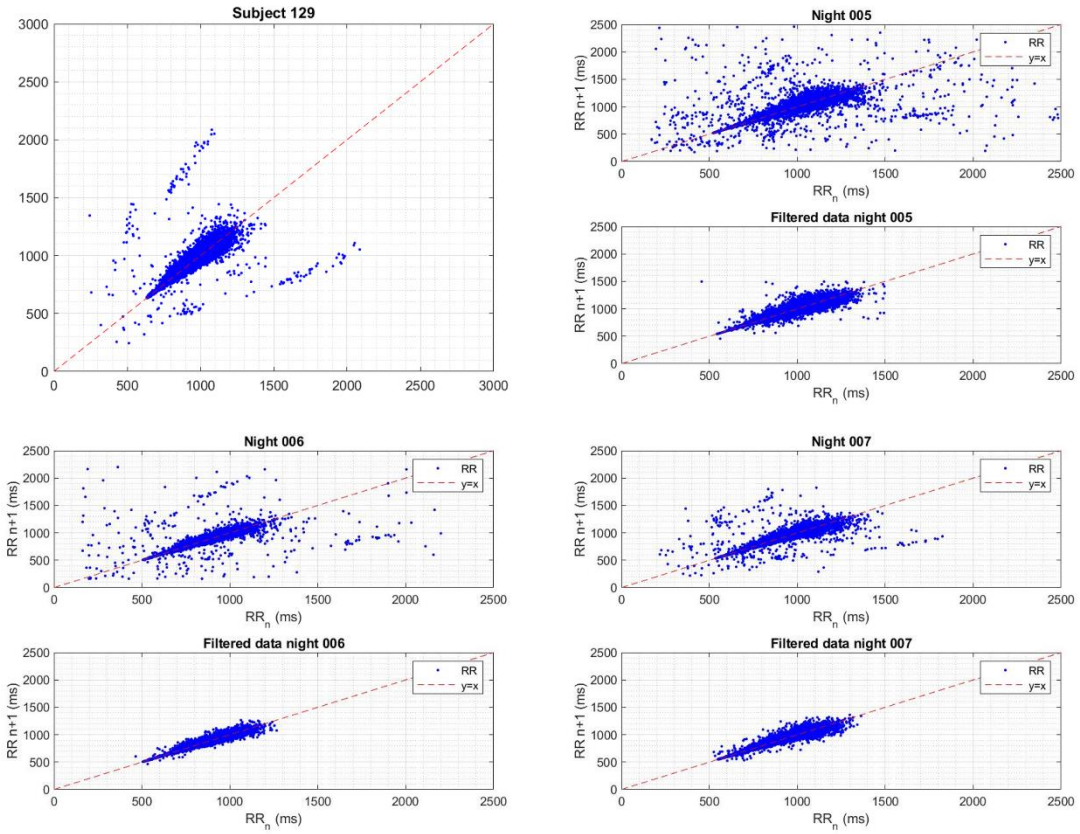

Figure A3. Poincaré plot of subject 129. Data acquired by the gel electrodes during the clinical study (top, left), and data acquired in the home setting (remainder).

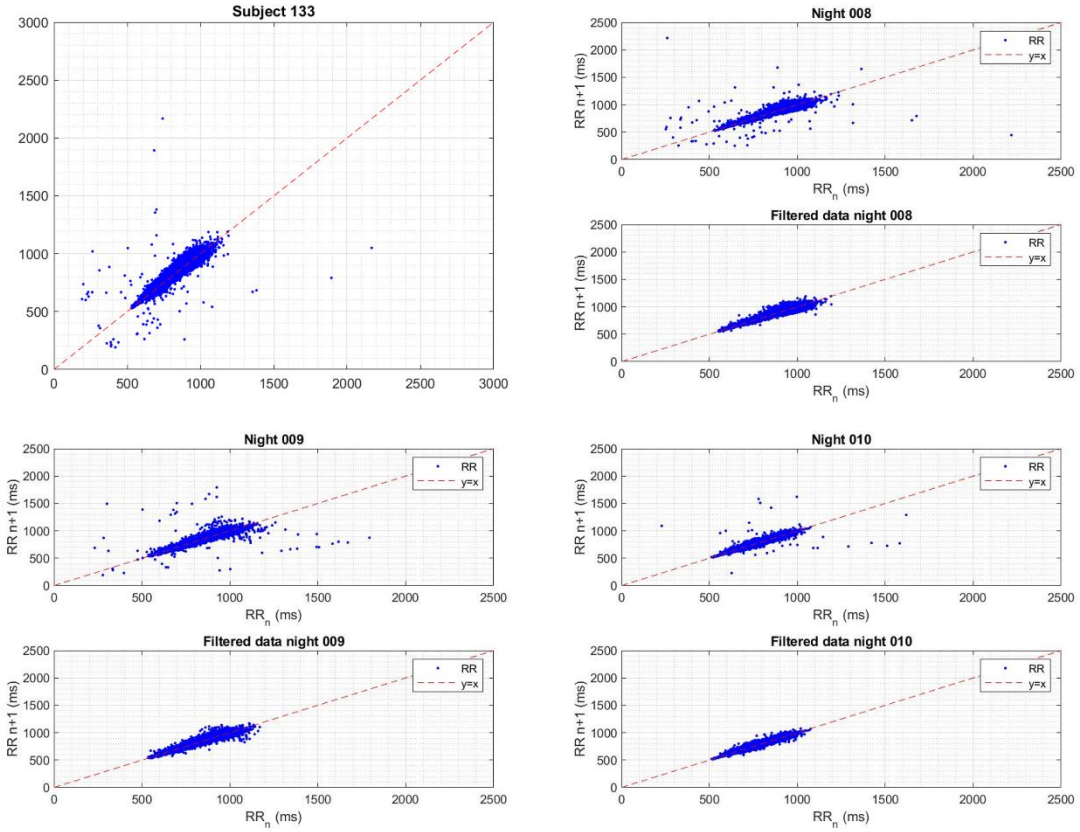

Figure A4. Poincaré plot of subject 133. Data acquired by the gel electrodes during the clinical study (top, left), and data acquired in the home setting (remainder).

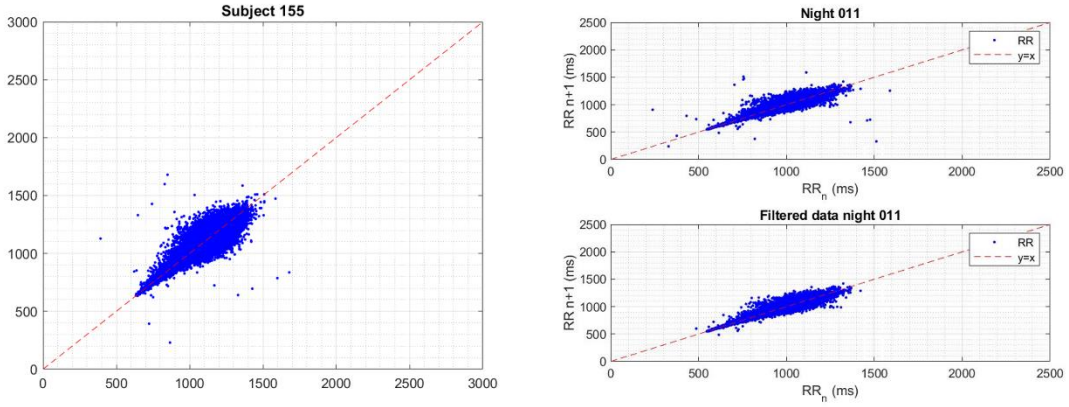

Figure A5. Poincaré plot of subject 155. Data acquired by the gel electrodes during the clinical study (left), and data acquired in the home setting (right).

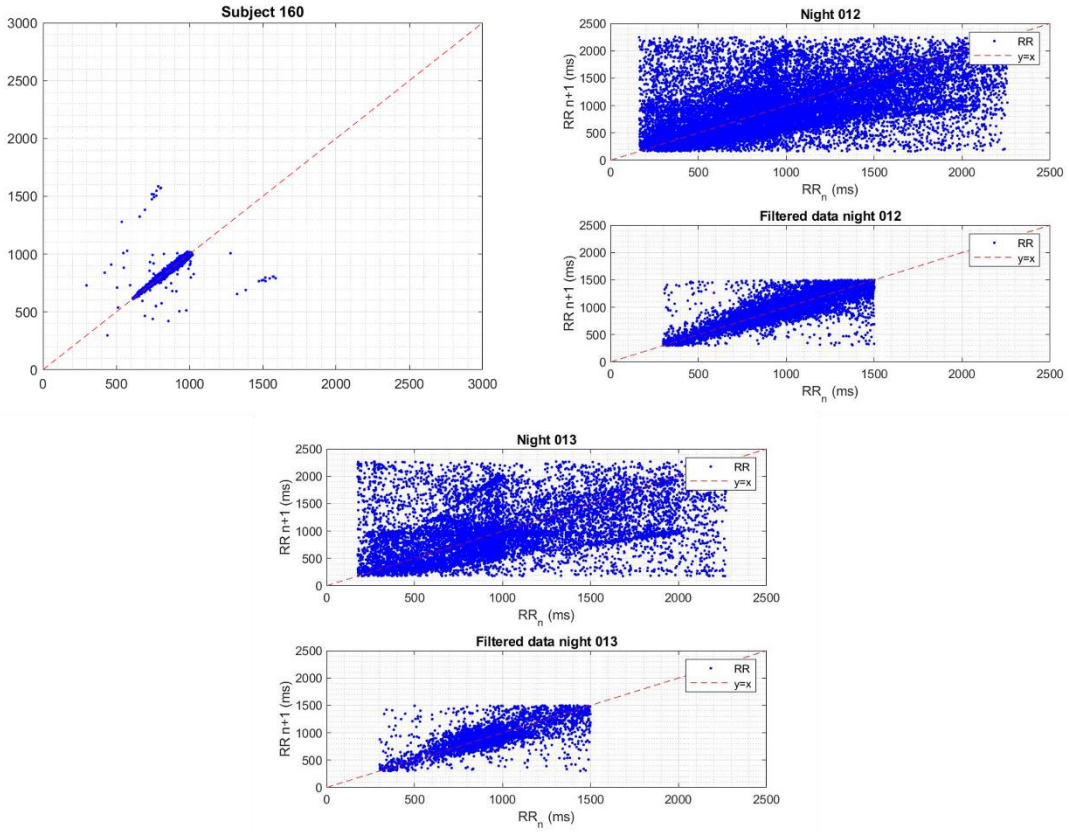

Figure A6. Poincaré plot of subject 160. Data acquired by the gel electrodes during the clinical study (top, left), and data acquired in the home setting (remainder).

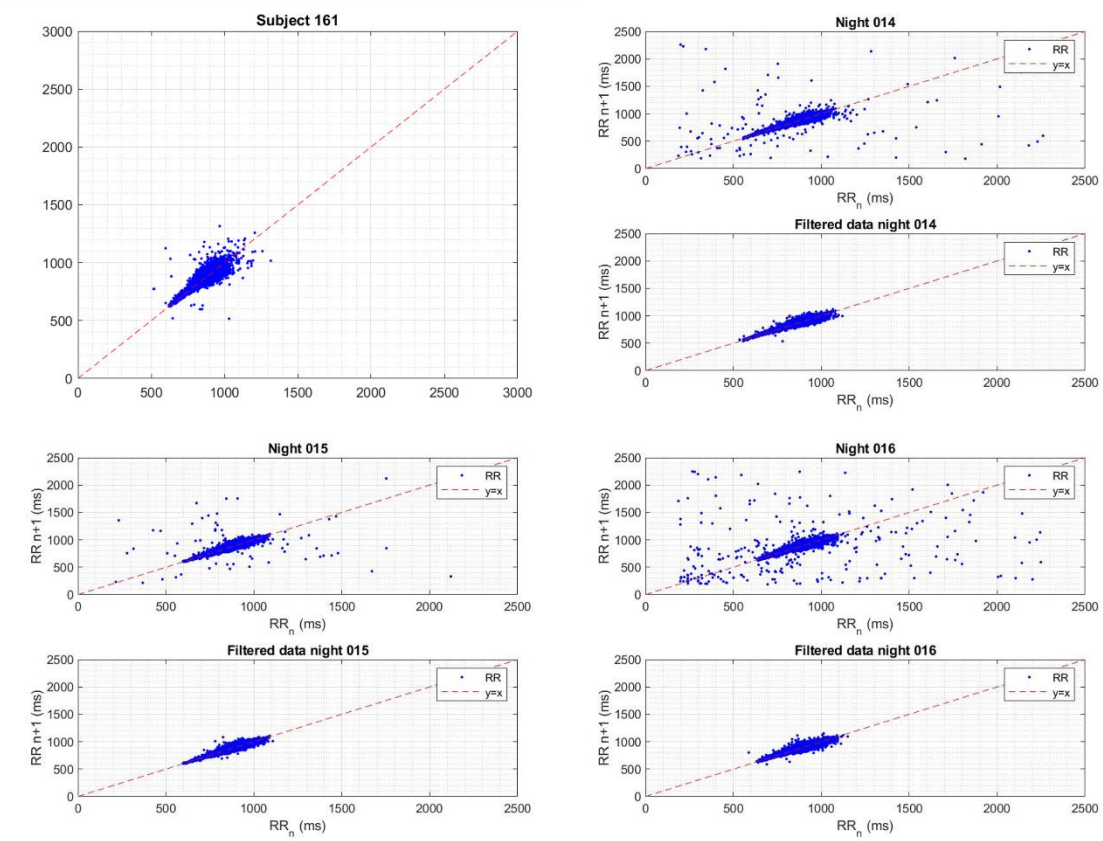

Figure A7. Poincaré plot of subject 161. Data acquired by the gel electrodes during the clinical study (top, left), and data acquired in the home setting (remainder).

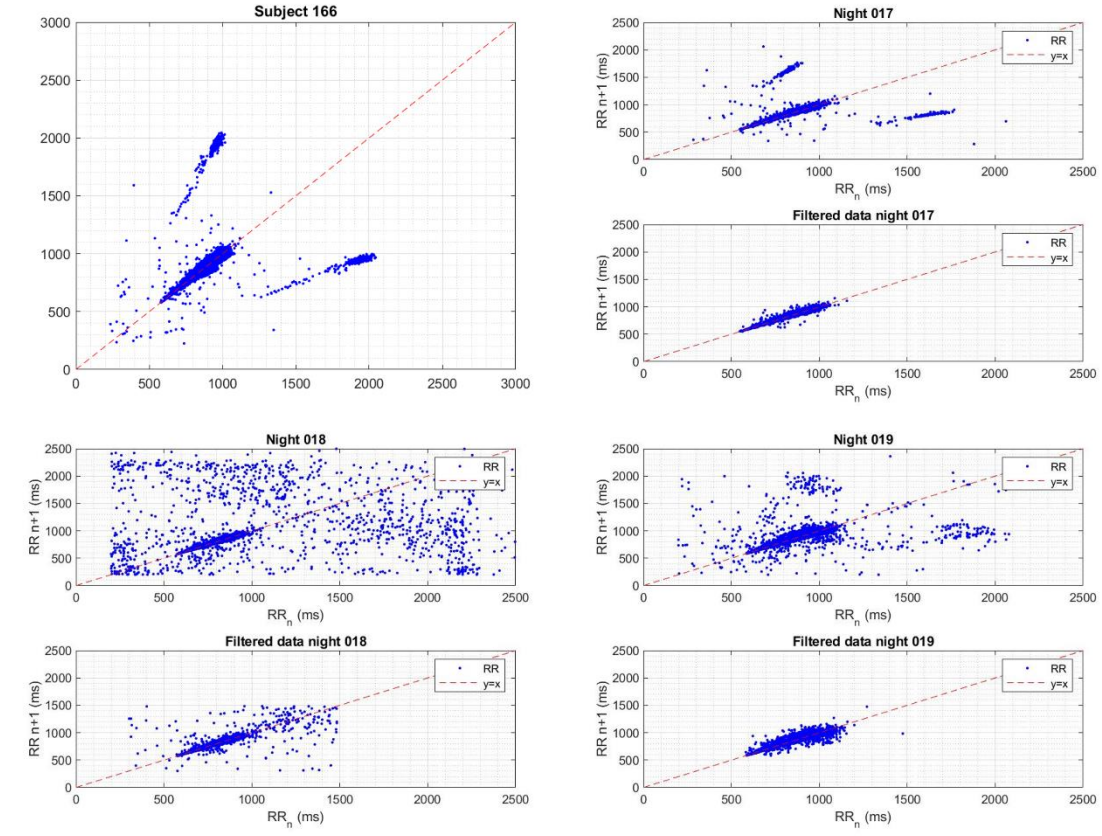

Figure A8. Poincaré plot of subject 166. Data acquired by the gel electrodes during the clinical study (top, left), and data acquired in the home setting (remainder).

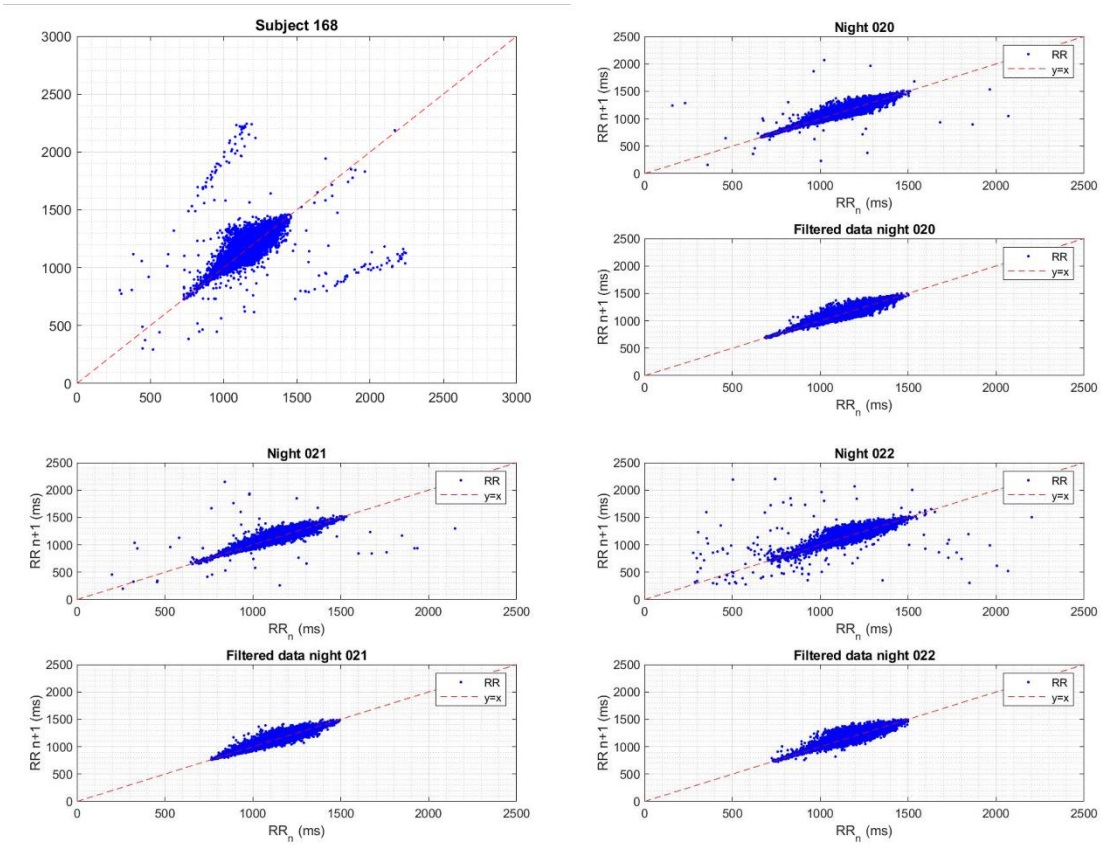

Figure A9. Poincaré plot of subject 168. Data acquired by the gel electrodes during the clinical study (top, left), and data acquired in the home setting (remainder).

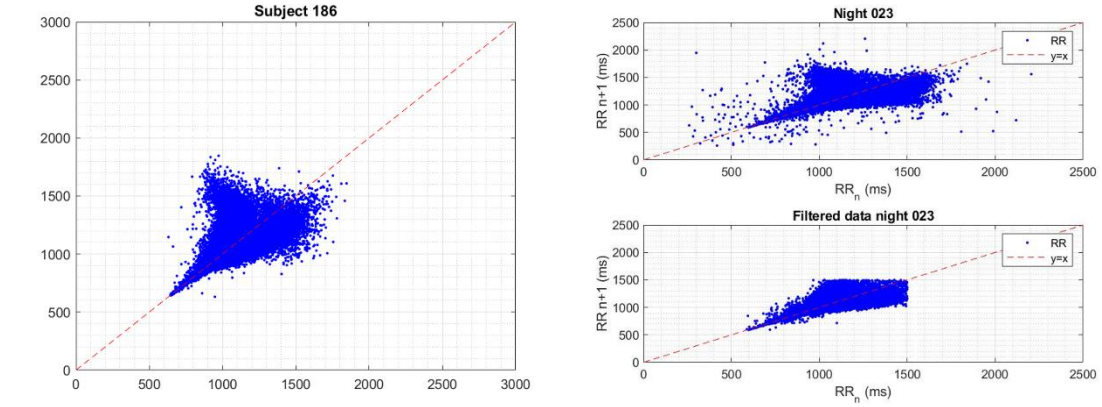

Figure A10. Poincaré plot of subject 186. Data acquired by the gel electrodes during the clinical study (left), and data acquired in the home setting (right).

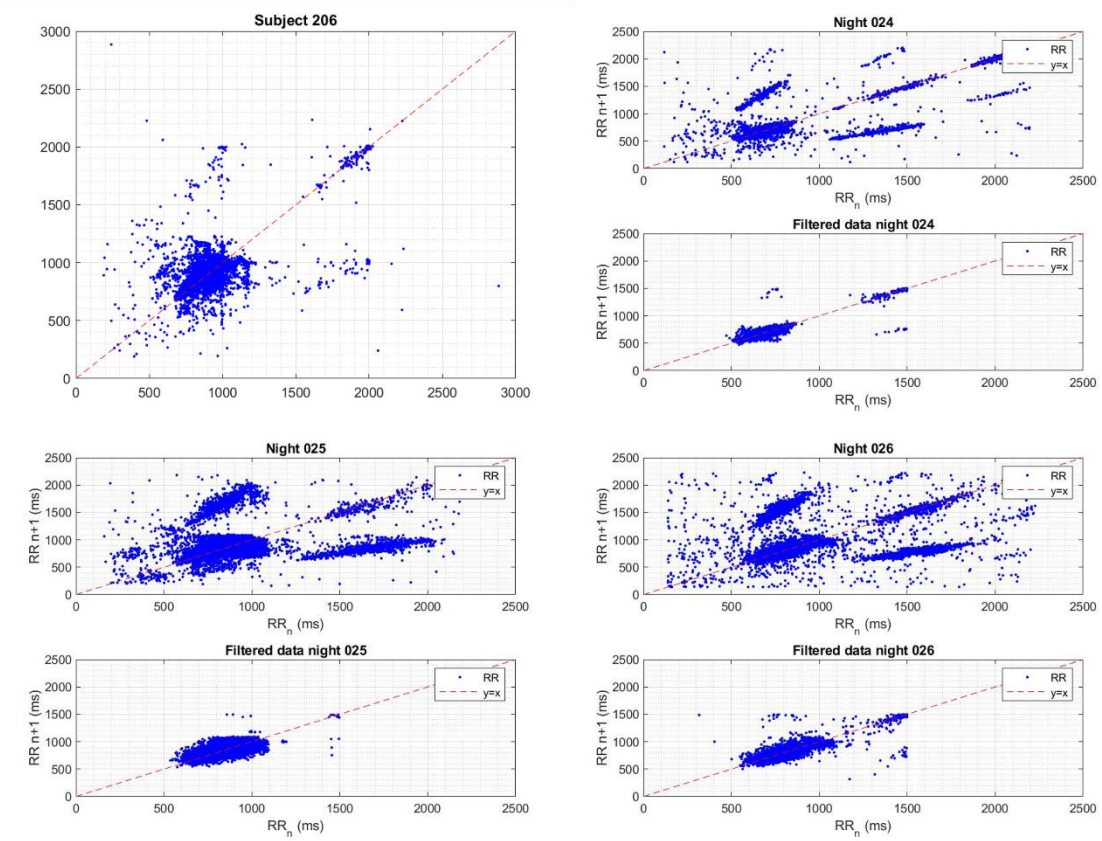

Figure A11. Poincaré plot of subject 206. Data acquired by the gel electrodes during the clinical study (top, left), and data acquired in the home setting (remainder).

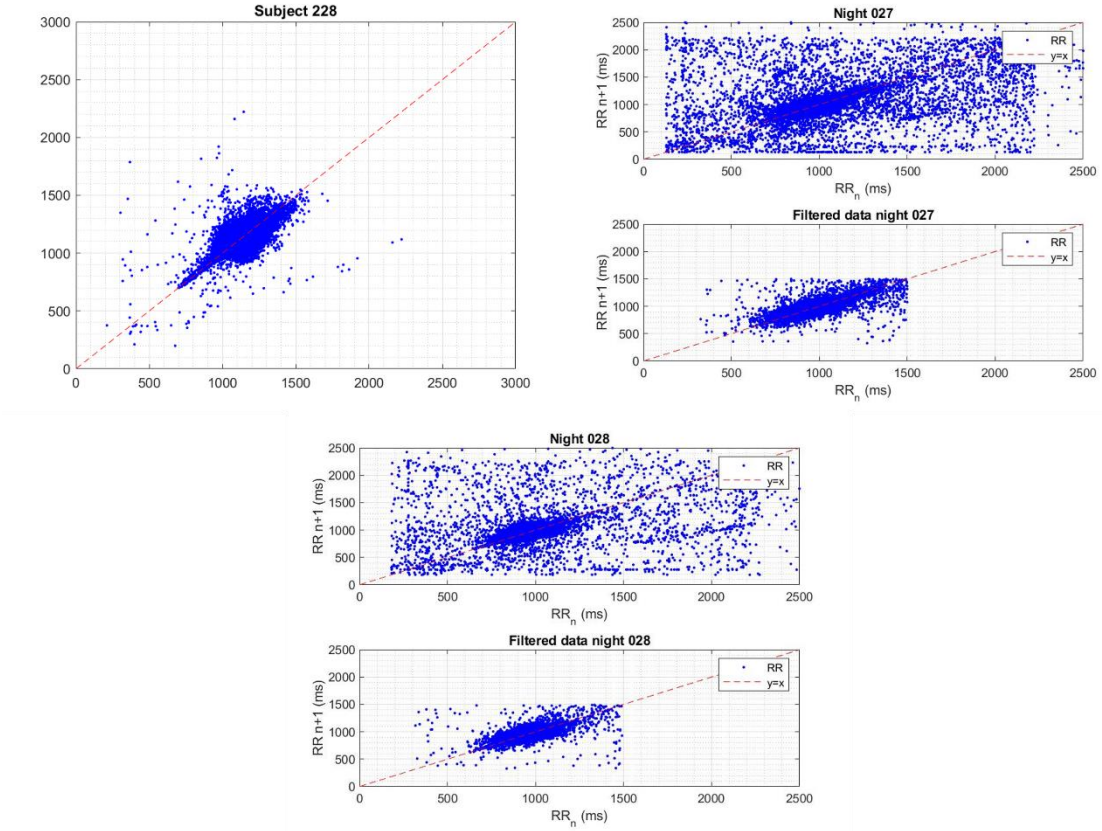

Figure A12. Poincaré plot of subject 228. Data acquired by the gel electrodes during the clinical study (top, left), and data acquired in the home setting (remainder).